

Technical report 17-008

A Multi-Class Model-Based Control Scheme for Reducing Congestion and Emissions in Freeway Networks by Combining Ramp Metering and Route Guidance*

C. Pasquale, S. Sacone, S. Siri, and B. De Schutter

To cite this work, please refer to the published version:

C. Pasquale, S. Sacone, S. Siri, and B. De Schutter, “A multi-class model-based control scheme for reducing congestion and emissions in freeway networks by combining ramp metering and route guidance,” *Transportation Research Part C*, vol. 80, pp. 348–408, July 2017. doi:[10.1016/j.trc.2017.04.007](https://doi.org/10.1016/j.trc.2017.04.007)

A multi-class model-based control scheme for reducing congestion and emissions in freeway networks by combining ramp metering and route guidance

C. Pasquale, S. Sacone, S. Siri

Department of Informatics, Bioengineering, Robotics and Systems Engineering, University of Genova, Italy

B. De Schutter

Delft Center for Systems and Control, Delft University of Technology, The Netherlands

Abstract

The paper proposes a multi-class control scheme for freeway traffic networks. This control scheme combines two control strategies, i.e. ramp metering and route guidance, in order to reduce the total time spent and the total emissions in a balanced way. In particular, the ramp metering and route guidance controllers are feedback predictive controllers, i.e. they compute the control actions not only on the basis of the measured system state, but also on the prediction of the system evolution, in terms of traffic conditions and fuel emissions. Another important feature of the controllers is that they have a multi-class nature: different classes of vehicles are considered and specific control actions are computed for each class. Since the controllers are based on a set of parameters that need to be tuned, the overall control framework also includes a module to properly determine the gains of the controllers. The simulation analysis reported in the paper shows the effectiveness of the proposed control framework and, in particular, the possibility of implementing control policies that are specific for each vehicle type.

Keywords: Freeway networks, Integrated control, Ramp metering, Route guidance, Predictive feedback controller, Fuel emissions

1. Introduction

Different traffic control strategies have been studied by researchers in the last decades in order to improve the travelling conditions of the drivers in freeway networks. Successful strategies are ramp metering, variable speed limits, route guidance, as well as combined strategies which are based on the application of different control measures Papageorgiou et al. (2003); Hegyi et al. (2009). In the present work, a multi-class and multi-objective combined ramp metering and routing control strategy is proposed for a freeway network, in order to reduce the total time spent and the total emissions in a balanced way.

Analysing the wide literature on freeway traffic control, it is worth noting that most of the research works are devoted to the sole reduction of congestion phenomena, i.e. to the minimisation of the total time spent by the

drivers in the traffic network, which has been proven to be equivalent to maximise the throughput in the system Papageorgiou and Kotsialos. (2002, 2004); Burger et al. (2013). However, in the last years, many other aspects have received great attention for enhancing the mobility of people and the quality of traffic systems, such as the reduction of pollutant emissions, noise, and environmental deterioration, as well as the increase of safety. Hence, also in the design of traffic control schemes for realising sustainable traffic systems, these environment-related aspects can be explicitly taken into consideration. For instance, in Zegeye et al. (2013); Liu et al. (2014a); Pasquale et al. (2015b), ramp metering or combined control strategies are studied to take into account the reduction of traffic congestion as well as the decrease of emissions. These objectives are also pursued by the controllers proposed in this paper which aim to balance the two objectives in a freeway network by means of proper ramp metering and routing control actions.

The combination of ramp metering and routing control strategies exploited in this paper is motivated by their high effectiveness in freeway networks. Ramp metering is one of the most common freeway traffic control strategies, which regulates the traffic flow entering the freeway mainstream by using traffic lights positioned at the on-ramps Papageorgiou and Papamichail. (2008). Route guidance is another common traffic control technique which has been broadly applied in large freeway networks to suggest the drivers the best paths to follow in specific traffic conditions Ben-Akiva et al. (2001). Many real applications have shown that ramp metering and routing control are effective strategies, which surely show their highest potential when combined together Kotsialos et al. (2002).

One of the features of the work developed in this paper is that different classes of vehicles are explicitly considered, i.e. cars, trucks, or specific vehicles, which present different dynamic behaviours and have different environmental impacts on the freeway system. In particular, not only the macroscopic dynamic model used in this paper to represent the evolution of the freeway network is of the multi-class type, but also the considered controllers are designed in order to define specific control actions for different vehicle classes. The idea of proposing a multi-class regulator is rather recent and has been developed in few research works, such as for instance in Pasquale et al. (2015b); Caligaris et al. (2007); Schreiter et al. (2011); Liu et al. (2017). It is important to emphasise that the use of a multi-class macroscopic model allows to represent the traffic system behaviour more accurately than with a one-class model which assumes that the whole traffic is a homogeneous fluid. This is true for instance in case a high percentage of trucks is present in the freeway traffic system, since trucks have a strong impact on the overall traffic flow for many reasons (because of their high dimensions and low operating capabilities, because their presence has a psychological impact on the drivers of nearby vehicles, and so on). Moreover, the use of a multi-class traffic model is particularly adequate for roads with multiple lanes, as it normally happens in freeways, in which fast vehicles can overtake slow vehicles, thus generating different flows sharing the same infrastructure.

In addition, setting separate control actions for the different classes of vehicles can represent a further opportunity to make the freeway traffic system perform more efficiently, for instance by assigning different priorities to the different vehicle categories. In practice, controlling separately the different vehicle classes via ramp metering means that separate lanes and signals must

be present at on-ramps, as it is already practised in some countries for cars and trucks New Zealand Transport Agency (2011); Burley and Gaffney. (2013). In the present work, we assume that the considered freeway is provided with dedicated on-ramps for each class of vehicles. As for route guidance, different indications must be given to the different vehicle typologies, normally displayed on Variable Message Signs (VMS). Note that the increasing availability of on-board devices enables the implementation of routing indications communicated to vehicles and further motivates the distinction of the traffic flow in different vehicle classes.

The design requirements of the proposed control scheme are the following:

- effective use of system state measurements and predictions;
- definition of dedicated control actions (ramp metering and route guidance) for different vehicle classes;
- improvement of the system performance defined as the combined reduction of travel times and traffic emissions;
- computational effort suitable for an on-line implementation.

To meet these requirements, a feedback predictive control scheme is designed in which the control action is computed on the basis of the measured system state and, also, on the prediction of the system evolution. The aim of the regulators is to reduce travel times and traffic emissions through specific control actions for different vehicle classes. Finally, the last requirement has led to the choice of a control scheme in which no on-line optimisation is required, differently from what has been done in other works (e.g. Karimi et al. (2004); Sacone and Siri. (2012); Muralidharan and Horowitz. (2015); Ferrara et al. (2015)) in which Model Predictive Control (MPC) techniques have been adopted. Indeed, in MPC schemes a large-scale nonlinear optimisation problem should be solved on-line, with a high computational load affordable only in small freeway networks.

The paper is organised as follows. In Section 2 a detailed literature review is carried out. Section 3 is devoted to present the multi-class macroscopic traffic model adopted in this paper, while the considered macroscopic VER-SIT+ emission model is analysed in Section 4. The proposed multi-class and multi-objective control framework is introduced in Section 5, while its main components, i.e. the controllers and the gains selector, are described in detail in Section 6 and in Section 7, respectively. Some simulation results are discussed in Section 8, and conclusive remarks are drawn in Section 9.

2. Literature review

In the following, a detailed review of the literature is reported for the main topics of the proposed work, i.e. multi-class traffic flow models, emission models, as well as ramp metering and route guidance control. The section ends with the detailed description of the paper contributions.

2.1. Multi-class traffic models

Multi-class traffic models have been proposed in the literature in order to represent the behaviours of different classes of vehicles, which can be identified

according to the type of vehicle (e.g. cars, trucks, public transport vehicles), the traveller characteristics (e.g. commuters, transport of goods), and so on. One of the first attempts to represent different types of vehicles in macroscopic traffic models is given by multi-lane models Holland and Woods. (1997); Daganzo. (1997), where two types of vehicles and a set of dedicated lanes are modelled through separate Lighthill-Whitham-Richards (LWR) models and separate fundamental diagrams. A macroscopic multi-class continuum traffic flow model, derived from mesoscopic principles, is reported in Hoogendoorn and Bovy. (2000), an extension of which can be found in Hoogendoorn and Bovy. (2001), where a gas-kinetic traffic flow model using a platoon-based multi-class description of traffic flow is proposed. Heterogeneous groups of drivers are also studied in Wong and Wong. (2002), where an extension of the LWR model is formulated and different speed distributions are defined for each class of road users. A further proposal is presented in Bagnerini and Rasche. (2003), where several types of vehicles are modelled through a homogenised hyperbolic traffic flow model. A more recent approach, again based on the kinematic wave theory, is proposed in Logghe and Immers. (2008), where new assumptions on the interactions among classes are introduced and a new multi-class LWR model is formulated. Finally, one of the most recent innovations in macroscopic first-order multi-class models is the Fastlane model, firstly introduced in Van Lint et al. (2008) and successively extended in Schreiter et al. (2011) to include traffic control measures.

Only few studies consider the extension of second-order macroscopic models to the multi-class context. In Deo et al. (2009), the METANET model Papageorgiou et al. (1990) is adapted to represent a heterogeneous flow, considering a simple interpolation between the different fundamental diagrams of each class of vehicles. A two-class extension of METANET is carried out also in Caligaris et al. (2010); Pasquale et al. (2014), in which the interaction between cars and trucks is appropriately modelled through a fundamental diagram, different for each class, in which the flow of each class depends on the densities of the two vehicle classes. A different multi-class second-order traffic model is proposed in Liu et al. (2014b), being inspired from Logghe and Immers. (2008).

2.2. Emission models

Analogously to the standard classification of traffic flow models, emission models may be classified in microscopic models (in which emission factors are computed according to an accurate description of the physical processes) Bachman et al. (2000); Ahn et al. (2002); Smit et al. (2005); Ligterink et al. (2009), macroscopic models (based on aggregate variables) Ntziachristos et al. (2000); Ntziachristos and Kouridis. (2007); U.S. Environmental Protection Agency. (2009); Hausberger et al. (2009); Joumard et al. (2007); Negrenti (1999), and mesoscopic models (with intermediate characteristics) Richardson and et al. (1981); Wallace et al. (1984).

Let us focus on *macroscopic* traffic emission models, that are interesting for this work where the traffic flow dynamics is described with a macroscopic model as well. Three categories of macroscopic emission models can be identified. The first group is constituted by “average-speed emission models”, which make an estimation of traffic emissions with a very low computational effort. These models compute the average value of the emission factors of each harmful substance, for different categories of vehicles, as a function of the average speed of the vehicle. The output produced by these models is a local emission factor, namely the mass of pollutant emitted per kilometre

and per vehicle. Some widely used average-speed emission models are COPERT Ntziachristos et al. (2000); Ntziachristos and Kouridis. (2007) and MOBILE U.S. Environmental Protection Agency. (2009), this latter requiring detailed information about the type of vehicle, the fuel, and the environmental conditions.

Another typology of macroscopic emission models is represented by “traffic-situation emission models”, which compute emissions and fuel consumptions according to specific traffic conditions. More specifically, these models receive as inputs several sets of driving patterns, reproducing the behaviour of different driving conditions (e.g. free-flow, congested, stop-and-go) and traffic scenarios (freeway, rural road, arterial road, urban road). Some common traffic-situation emission models are for instance HBEFA Hausberger et al. (2009) and ARTEMIS Joumard et al. (2007).

The third category is represented by “traffic-variable emission models”. The emission factors generated by these models depend on the average dynamic traffic variables (speed, density, flow and queue length) and on the characteristics of the transport infrastructures. In addition, in order to consider the variance of traffic variables, some correction factors are introduced. An example of such models can be found in Negrenti (1999).

The model adopted in this work is a macroscopic version of VERSIT+ Smit et al. (2005), which belongs to the class of regression-based models of microscopic type. VERSIT+ allows to compute many types of pollutant emissions for a wide range of vehicles and for several traffic conditions. In the original version of the model, the prediction of the emission factor was exclusively dependent on the average speed, but, in order to achieve a more accurate estimation, Ligterink et al. (2009) proposes an improved version of VERSIT+ , that includes the average acceleration for the prediction. The macroscopic extension of VERSIT+ has been introduced in Zegeye et al. (2013), while its use in a multi-class traffic framework can be found in Liu et al. (2014a); Pasquale et al. (2015a, 2016b).

2.3. Ramp metering and route guidance control

Traffic control techniques for reducing congestion phenomena in freeway systems have been studied by researchers for some decades. Most of them are based on *ramp metering*. For instance, the simple ramp metering strategy ALINEA Papageorgiou et al. (1991), a feedback traffic controller developed in the late Eighties, has been successfully applied worldwide. During the years, different variations of ALINEA have been proposed Papamichail et al. (2007), such as the proportional-integral version PI-ALINEA Wang et al. (2010), which has been proven to be more effective than ALINEA for specific cases such as distant downstream bottlenecks Wang et al. (2014). Besides these simple controllers, different and more sophisticated ramp metering control approaches have been studied, based on optimisation or optimal control techniques Burger et al. (2013); Gomes and Horowitz. (2006). For instance, Papageorgiou and Kotsialos. (2004) describes the optimal freeway traffic control tool AMOC, based on a numerical solution algorithm for nonlinear optimal control problems, while Bellemans et al. (2006) proposes a ramp metering scheme based on a nonlinear MPC approach. However, these optimisation-based traffic controllers are hardly applicable in large freeway networks for real-time uses because of their computational complexity, hence computationally efficient MPC approaches are sought Muralidharan and Horowitz.

(2015). In order to deal with these aspects, distributed freeway control approaches have been recently investigated Ferrara et al.; Pisarski and Canudas de Wit. (2016), as well as event-triggered MPC schemes Ferrara et al. (2015).

Only few and recent research works in the literature deal with the design of ramp metering controllers to reduce traffic emissions. For instance, in Zegeye et al. (2012), the authors propose a parameterised MPC approach where the control objective is a weighted sum of travel times, emissions, and the variances in the control signals, while the same authors in Zegeye et al. (2013) propose a general traffic control framework to integrate macroscopic traffic flow models and microscopic emission and fuel consumption models. A dispersion model for motorway traffic emissions is investigated in Csikós et al. (2015) for control purposes, whereas Liu et al. (2013) describes an MPC approach to determine a ramp metering action aimed at jointly reducing traffic emissions and travel times in single freeway stretches. A two-class freeway traffic controller to reduce congestion and emissions is also presented in Pasquale et al. (2015b), by exploiting optimal control techniques for the solution of the resulting multi-objective nonlinear optimal control problem.

Route guidance is an effective traffic control technique that can be applied in freeway networks where the drivers have to choose among alternative paths. In Pavlis and M.Papageorgiou. (1999); Wang et al. (2001) a classification of the routing control strategies is reported, by distinguishing two categories: feedback strategies, where the routing problem is solved taking into account the instantaneous travel time along the selected paths, and iterative strategies, that use real-time measurements and disturbance predictions, to provide the exact solution of the problem. Although this last type of approach is very efficient, it requires a high computational effort; for this reason, the authors of Wang et al. (2002) propose a predictive feedback strategy that incorporates the advantages of feedback and iterative strategies. Other approaches consider fuzzy systems Wahle et al. (2001); Henn. (2000); Pang et al. (1999), or Mixed Integer Linear Programming formulations to solve cooperative problems of route guidance Kaufman et al. (1998), or the variational inequality paradigm for the ideal dynamic user optimal route choice problem W.Jang et al. (2005). In the context of freeway traffic systems, some approaches regard the application of route guidance combined with other control strategies, for example in Karimi et al. (2004), where the routing problem is combined with ramp metering within an MPC approach, or in Kotsialos et al. (2002), where a discrete-time constrained nonlinear optimal control problem is solved for a case in which route guidance is combined with ramp metering and motorway-to-motorway control.

Only few contributions on routing strategies deal with environmental issues. In Tzeng and Chen. (1993), a multi-objective approach is proposed in order to define the optimal flows that minimise the total travel time, the travel distance and the pollutant emissions. In Venigalla et al. (1999), the defined routing algorithm evaluates the environmental impact of the traffic system by considering the operating conditions of vehicles along the assigned route. Moreover, in Ahn and Rakha. (2008) the environmental and energetic impacts produced by the route choice decisions are defined by using both a microscopic and a macroscopic simulator, while in Rakha et al. (2012) two eco-routing algorithms based on feedback assignment are proposed. In Luo et al. (2016) an MPC framework for real-time en-route diversion control is proposed to improve traffic efficiency, while reducing emissions and fuel consumptions: Tabu Search is applied to solve

the resulting optimisation problems.

2.4. Contributions of the paper

In the current paper, the adopted traffic model is METANET for freeway networks in the destination-oriented mode, properly extended to take into account the multi-class case. The interaction among different types of vehicles is modelled analogously to Caligaris et al. (2010); Pasquale et al. (2014), where only a freeway stretch is considered. This traffic model for multi-class freeway networks is original and presented in this paper for the first time (a preliminary version of this model, with a different notation, is reported in Pasquale et al. (2016b)).

Also the emission model adopted in this paper is original. In particular, such a model is VERSIT+ for multi-class freeway networks including the computation of emissions at the on-ramps. This model extends to freeway networks the one proposed in Pasquale et al. (2015a), which was referred to a freeway stretch.

The main contribution of the present work stands in the traffic control framework. The multi-class routing control strategy proposed in this paper is inspired by Wang et al. (2002), i.e. it is a feedback strategy which computes the control action on the basis of the measured system state and, also, on the prediction of the system evolution. This prediction is realised by on-line running a proper simulation model in order to predict travel times and traffic emissions over a given horizon. Compared to Wang et al. (2002), the present paper proposes a *multi-class* control scheme based on the predicted total travel time and the *predicted total emissions*, whereas in Wang et al. (2002) only the predicted total time is considered in presence of only one class of vehicles. Moreover, in the current paper, route guidance is combined with a *multi-class feedback ramp-metering* strategy in order to further reduce emissions and congestion in freeway networks. The adopted ramp metering controller is the multi-class PI-ALINEA feedback controller, whose effectiveness has already been analysed for a freeway stretch where only ramp metering is applied Pasquale et al. (2014).

A preliminary version of the control scheme described in this paper has been defined in Pasquale et al. (2016b). In particular, the control framework proposed in the present work extends the one in Pasquale et al. (2016b), since the route guidance controller is *more general* (considering more than two paths for each origin-destination pair, adding penalising factors for representing specific emission restriction policies, and so on) and a suitable *controller gains selector* procedure is introduced to fix the controller gains on the basis of the present traffic conditions. Moreover, a deeper simulation analysis is performed in this paper to show the effectiveness and versatility of the proposed controller.

3. The multi-class network traffic model

As previously introduced, the considered traffic flow model is based on METANET Papageorgiou et al. (1990), in the destination-oriented mode, properly extended to the multi-class case. In the considered model, the freeway system is represented by means of a directed graph, shown in Fig. 1, composed of:

- M freeway links, modelling the traffic behaviour in homogeneous freeway stretches;
- O origin links, modelling the links which forward traffic volumes from outside the network into the considered freeway; among these origin links there are also on-ramps that can be controlled via ramp metering;
- N nodes, characterised by no more than three links (in case of more complex nodes, they are decomposed in nodes meeting such condition by introducing dummy links and dummy nodes).

”place Fig. 1 about here”

Each freeway link $m = 1, \dots, M$ is further divided into N_m sections with length L_m and λ_m lanes. Moreover, the set of destinations reachable from link m is denoted as J_m . Analogously, \bar{J}_o is the set of destinations reachable from origin link $o = 1, \dots, O$. Also, for each node $n = 1, \dots, N$, \bar{J}_n is the set of reachable destinations, O_n is the set of exiting links, and I_n, \bar{I}_n are the set of entering freeway links and entering origin links, respectively.

The time horizon is divided into K time steps, with sample time interval T [h], and C classes of vehicles are considered. In order to correctly model the presence of different types of vehicles, let us introduce the parameter η^c , $c = 1, \dots, C$, which represents a conversion factor of vehicles of class c in cars. This parameter has a meaning analogous to the definition of passenger car equivalents (PCE), that is the number of passenger cars displaced by a single heavy vehicle of a particular type under specific traffic and control conditions National Research Council (1994).

The main variables referring to the freeway links are:

- $\rho_{m,i,j}^c(k)$ is the partial traffic density of class c in section i of link m at time instant kT with destination $j \in J_m$ [veh of class c /km/lane];
- $\rho_{m,i}^c(k)$ is the traffic density of class c in section i of link m at time instant kT [veh of class c /km/lane];
- $\rho_{m,i}(k)$ is the total traffic density in section i of link m at time instant kT [PCE/km/lane];
- $v_{m,i}^c(k)$ is the mean traffic speed of class c in section i of link m at time instant kT [km/h];
- $q_{m,i}^c(k)$ is the traffic volume of class c leaving section i of link m during time interval $[kT, (k+1)T)$ [veh of class c /h];
- $\gamma_{m,i,j}^c(k)$ is the portion of the traffic volume of class c in section i of link m at time instant kT having destination $j \in J_m$ (composition rate).

The main variables referring to the origin links are:

- $d_{o,j}^c(k)$ is the partial origin demand of class c entering origin link o at time instant kT with destination $j \in \bar{J}_o$ [veh of class c /h];

- $d_o^c(k)$ is the origin demand of class c entering origin link o at time instant kT [veh of class c/h];
- $l_{o,j}^c(k)$ is the partial queue length of class c at origin link o with destination $j \in \bar{J}_o$ at time instant kT [veh of class c];
- $l_o^c(k)$ is the queue length of class c at origin link o at time instant kT [veh of class c];
- $\gamma_{o,j}^c(k)$ is the portion of the traffic volume of class c leaving origin link o at time instant kT having destination $j \in \bar{J}_o$ (composition rate);
- $\theta_{o,j}^c(k)$ is the portion of the demand of class c originating in origin link o at time instant kT having destination $j \in \bar{J}_o$;
- $q_o^c(k)$ is the traffic volume of class c leaving origin link o during time interval $[kT, (k+1)T)$ [veh of class c/h];
- $q_o(k)$ is the total traffic volume leaving origin link o during time interval $[kT, (k+1)T)$ [PCE/h].

The variables referring to the nodes are:

- $Q_{n,j}^c(k)$ is the flow of class c entering node n during time interval $[kT, (k+1)T)$ with destination $j \in \bar{J}_n$ [veh of class c/h];
- $\beta_{m,n,j}^c(k)$ is the splitting rate, i.e. the portion of the traffic volume present in node n at time instant kT which chooses link m to reach destination $j \in \bar{J}_n$.

Starting from the *freeway links*, a first dynamic equation is written for the partial traffic density, i.e.

$$\rho_{m,i,j}^c(k+1) = \rho_{m,i,j}^c(k) + \frac{T}{L_m \lambda_m} \left[\gamma_{m,i-1,j}^c(k) q_{m,i-1}^c(k) - \gamma_{m,i,j}^c(k) q_{m,i}^c(k) \right] \quad (1)$$

$c = 1, \dots, C$, $m = 1, \dots, M$, $i = 1, \dots, N_m$, $j \in J_m$, $k = 0, \dots, K-1$, where $\gamma_{m,i,j}^c(k) = \frac{\rho_{m,i,j}^c(k)}{\rho_{m,i}^c(k)}$ and $\rho_{m,i}^c(k) = \sum_{j \in J_m} \rho_{m,i,j}^c(k)$.

The second state equation regards the dynamics of the traffic mean speed, i.e.

$$v_{m,i}^c(k+1) = v_{m,i}^c(k) + \frac{T}{\tau^c} \left[V^c(\rho_{m,i}(k)) - v_{m,i}^c(k) \right] + \frac{T}{L_m} v_{m,i}^c(k) \left[v_{m,i-1}^c(k) - v_{m,i}^c(k) \right] - \frac{\nu^c T [\rho_{m,i+1}(k) - \rho_{m,i}(k)]}{\tau^c L_m [\rho_{m,i}(k) + \chi^c]} \quad (2)$$

$c = 1, \dots, C$, $m = 1, \dots, M$, $i = 1, \dots, N_m$, $k = 0, \dots, K-1$, where τ^c , ν^c , χ^c are model parameters referred to class c . The steady-state speed-density relation $V^c(\rho_{m,i}(k))$ is obtained as

$$V^c(\rho_{m,i}(k)) = v_{m,i}^{f,c} \cdot \left[1 - \left(\frac{\rho_{m,i}(k)}{\rho_{m,i}^{\max}} \right)^{l^c} \right]^{m^c} \quad (3)$$

where $v_{m,i}^{f,c}$ is the free-flow speed in section i of link m for class c [km/h], $\rho_{m,i}^{\max}$ is the jam density in section i of link m [PCE/km/lane], whereas l^c , m^c are other model parameters.

The total density is computed as

$$\rho_{m,i}(k) = \sum_{c=1}^C \eta^c \rho_{m,i}^c(k) \quad (4)$$

while the traffic volume is obtained as

$$q_{m,i}^c(k) = \rho_{m,i}^c(k) v_{m,i}^c(k) \lambda_m \quad (5)$$

In (2) a further additional term can be added to take into account the speed reduction caused by merging phenomena near on-ramps. In particular, consider a node in which a freeway link merges with an origin link o ; in the first section of link m leaving that node there is a speed reduction given by

$$-\Delta^c T \frac{v_{m,1}^c(k) q_o(k)}{L_m \lambda_m [\rho_{m,1}(k) + \chi^c]} \quad (6)$$

where Δ^c is a constant parameter defined for class c .

In (2) boundary conditions are needed, i.e. the virtual downstream density at the end of the link $\rho_{m,N_m+1}(k)$ and the virtual upstream speed at the beginning of the link $v_{m,0}^c(k)$. If node n (at the end of link m) has more than one leaving link, the virtual downstream density can be computed as

$$\rho_{m,N_m+1}(k) = \frac{\sum_{\mu \in O_n} (\rho_{\mu,1}(k))^2}{\sum_{\mu \in O_n} \rho_{\mu,1}(k)} \quad (7)$$

In case node n (at the beginning of link m) has more than one entering link, the virtual upstream speed may be computed as

$$v_{m,0}^c(k) = \frac{\sum_{\mu \in I_n} v_{\mu,N_\mu}^c(k) q_{\mu,N_\mu}^c(k)}{\sum_{\mu \in I_n} q_{\mu,N_\mu}^c(k)} \quad (8)$$

Let us now consider the *origin links*. The dynamic evolution of the partial queue length is calculated as

$$l_{o,j}^c(k+1) = l_{o,j}^c(k) + T [d_{o,j}^c(k) - \gamma_{o,j}^c(k) q_o^c(k)] \quad (9)$$

$c = 1, \dots, C$, $o = 1, \dots, O$, $j = 1, \dots, \bar{J}_o$, $k = 0, \dots, K-1$, with $\gamma_{o,j}^c(k) = \frac{l_{o,j}^c(k)}{l_o^c(k)}$, $l_o^c(k) = \sum_{j \in \bar{J}_o} l_{o,j}^c(k)$, and $d_{o,j}^c(k) = \theta_{o,j}^c(k) d_o^c(k)$.

The traffic flow of class c leaving each origin link o , having m as downstream link, is given by

$$q_o^c(k) = \min \left\{ d_o^c(k) + \frac{l_o^c(k)}{T}, q_o^{\max,c}, q_o^{\max,c} \cdot \frac{\rho_{m,1}^{\max} - \rho_{m,1}(k)}{\rho_{m,1}^{\max} - \rho_{m,1}^{cr}} \right\} \quad (10)$$

where $d_o^c(k) = \sum_{j \in \bar{J}_o} d_{o,j}^c(k)$, $q_o^{\max,c}$ is the maximum flow of class c in origin link o , and $\rho_{m,1}^{\text{cr}}$ is the critical density of the first section of link m [PCE/km/lane]. This critical density $\rho_{m,1}^{\text{cr}}$ is obtained by calibrating a fundamental diagram, i.e. a steady-state relation of the total flow depending on the total density $\rho_{m,1}$, of the form

$$Q(\rho_{m,1}) = v_{m,1}^f \cdot \rho_{m,1} \cdot \left[1 - \left(\frac{\rho_{m,1}}{\rho_{m,1}^{\max}} \right)^l \right]^m \quad (11)$$

where $v_{m,1}^f$, $\rho_{m,1}^{\max}$, l , m are the parameters to be estimated through an identification procedure. The critical density $\rho_{m,1}^{\text{cr}}$ is then obtained as the value of $\rho_{m,1}$ corresponding to the maximum value of $Q(\rho_{m,1})$.

In case the considered origin link o is a controlled on-ramp, by denoting with $\bar{q}_o^c(k)$ the on-ramp flow computed by the controller for class c , the leaving traffic flow is given by

$$q_o^c(k) = \min \left\{ d_o^c(k) + \frac{l_o^c(k)}{T}, q_o^{\max,c}, \bar{q}_o^c(k), q_o^{\max,c} \cdot \frac{\rho_{m,1}^{\max} - \rho_{m,1}(k)}{\rho_{m,1}^{\max} - \rho_{m,1}^{\text{cr}}} \right\} \quad (12)$$

As for the *node* model, the incoming traffic flow is computed as

$$Q_{n,j}^c(k) = \sum_{\mu \in I_n} q_{\mu,N_\mu}^c(k) \cdot \gamma_{\mu,N_\mu,j}^c(k) + \sum_{o \in I_n} q_o^c(k) \cdot \gamma_{o,j}^c(k) \quad (13)$$

The traffic flow entering the first section of a link exiting a node is calculated as

$$q_{m,0}^c(k) = \sum_{j \in J_m} \beta_{m,n,j}^c(k) \cdot Q_{n,j}^c(k) \quad (14)$$

Note that the splitting rates must guarantee that $\sum_{\mu \in O_n} \beta_{\mu,n,j}^c(k) = 1$, $c = 1, \dots, C$, $n = 1, \dots, N$, $j \in \bar{J}_n$, $k = 0, \dots, K - 1$. In presence of control actions, the splitting rates are modelled by

$$\beta_{m,n,j}^c(k) = (1 - \varepsilon_{m,n}^c) \beta_{m,n,j}^{\text{N},c}(k) + \varepsilon_{m,n}^c \beta_{m,n,j}^{\text{C},c}(k) \quad (15)$$

where $\beta_{m,n,j}^{\text{N},c}(k)$ is the splitting rate without route recommendations properly computed on the basis of historical data, $\beta_{m,n,j}^{\text{C},c}(k)$ is the splitting rate defined with a suitable control approach, and $\varepsilon_{m,n}^c$ is the compliance rate with the route recommendations, $0 \leq \varepsilon_{m,n}^c \leq 1$.

The model presented in this section contains a number of parameters which must be properly calibrated. Hence, an identification procedure based on real traffic data should be realised off-line to calibrate all the model parameters of the considered freeway network. This identification procedure is not a trivial issue, both due to the large size of the considered system and due to the nonlinearities present in the traffic model. The interested reader can refer to a recent work on macroscopic traffic flow model calibration, i.e. Spiliopoulou et al. (2015), in which different optimisation algorithms, both stochastic and deterministic, are tested and compared.

4. The VERSIT+ emission model

In order to properly compute the freeway traffic emissions in the network, a multi-class macroscopic emission model is considered starting from the microscopic emission model VERSIT+. In the following, the microscopic VERSIT+ model is described and its extension to the macroscopic multi-class case for a freeway network is also reported.

4.1. The microscopic VERSIT+ emission model

According to the microscopic VERSIT+ emission model Ligterink et al. (2009), the emission factor of a given vehicle depends both on the value of its speed v [km/h] and on the combination of its acceleration a [m/s²] and speed, through the variable w defined as

$$w = a + 0.014v \quad (16)$$

Four driving conditions are identified, corresponding respectively to idling conditions, with $v < 5$ and $a < 0.5$, urban driving with $v \leq 50$, rural driving with $50 < v \leq 80$ and motorway driving with $v > 80$.

The emission factor E [g/s] is given by

$$E = \begin{cases} u_0 & \text{if } v < 5 \text{ and } a < 0.5 \\ u_1 + u_2 w_+ + u_3 (w - 1)_+ & \text{if } (5 \leq v \leq 50) \text{ or } (v < 5 \text{ and } a \geq 0.5) \\ u_4 + u_5 w_+ + u_6 (w - 1)_+ & \text{if } 50 < v \leq 80 \\ u_7 + u_8 (w - 0.5)_+ + u_9 (w - 1.5)_+ & \text{if } v > 80 \end{cases} \quad (17)$$

where u_h , $h = 0, \dots, 9$, are specific coefficients of the emission model. Moreover, the function $(x)_+$ projects x on the set of nonnegative numbers, i.e. $(x)_+ = 0$ if $x < 0$, and $(x)_+ = x$ otherwise.

4.2. The multi-class macroscopic VERSIT+ emission model

In order to adopt the VERSIT+ emission model for freeway networks, it is first of all necessary to extend the macroscopic multi-class traffic flow model described in Section 3 in order to compute the average acceleration and the number of vehicles for each link, for each class of vehicles and for every simulation time step. In Zegeye et al. (2013), two types of acceleration have been identified, i.e. the segmental acceleration considering the speed variation within a section, and the cross-segmental acceleration, which concerns the speed variation of vehicles moving from one section to the next one between two consecutive time steps. In Liu et al. (2014a) such accelerations have been extended to the multi-class case, while in Pasquale et al. (2015a) the model has been extended to add the computation of the emissions at the on-ramps. In the following, the proposed macroscopic multi-class VERSIT+ emission model for traffic networks is described.

In the *freeway links*, two types of acceleration are considered:

- the segmental acceleration $a_{m,i}^{\text{seg},c}(k)$ referring to vehicles of class c in section i of link m between time step k and time step $k+1$ (the number of vehicles subject to this acceleration is denoted as $n_{m,i}^{\text{seg},c}(k)$);
- the cross-segmental acceleration $a_{m,i,i+1}^{\text{cross},c}(k)$ of vehicles of class c moving from section i to section $i+1$ of link m between time step k and $k+1$ (the number of vehicles involved is indicated with $n_{m,i,i+1}^{\text{cross},c}(k)$).

The segmental acceleration is computed as

$$a_{m,i}^{\text{seg},c}(k) = \frac{v_{m,i}^c(k+1) - v_{m,i}^c(k)}{T} \quad (18)$$

while the cross-segmental acceleration is given by

$$a_{m,i,i+1}^{\text{cross},c}(k) = \frac{v_{m,i,i+1}^c(k+1) - v_{m,i}^c(k)}{T} \quad (19)$$

Note that at the boundary between two adjacent links, i.e. when vehicles move between the last section of a link and the first section of the downstream link, (19) still holds with a slightly different notation.

Moreover, the number of vehicles subject to these accelerations is respectively given by

$$n_{m,i}^{\text{seg},c}(k) = L_m \rho_{m,i}^c(k) - T q_{m,i}^c(k) \quad (20)$$

$$n_{m,i,i+1}^{\text{cross},c}(k) = T q_{m,i}^c(k) \quad (21)$$

In order to compute the pollutant emissions in the *origin links*, four types of acceleration are considered:

- the acceleration $a_o^{\text{a},c}(k)$ of arriving vehicles, i.e. vehicles of class c arriving at the origin link o at k and waiting in queue at $k+1$ (let $n_o^{\text{a},c}(k)$ indicate the number of arriving vehicles);
- the acceleration $a_o^{\text{w},c}(k)$ of waiting vehicles, i.e. vehicles of class c moving within the queue of the origin link o between k and $k+1$ (let $n_o^{\text{w},c}(k)$ indicate the number of waiting vehicles);
- the acceleration $a_o^{\text{ls},c}(k)$ of leaving vehicles with stop, i.e. vehicles of class c being in the queue of the origin link o at k and exiting link o at $k+1$ (let $n_o^{\text{ls},c}(k)$ indicate the number of leaving vehicles with stop);
- the acceleration $a_o^{\text{lns},c}(k)$ of leaving vehicles without stop, i.e. vehicles of class c arriving at the origin link o at k and exiting link o at $k+1$ without any intermediate stop in the queue (let $n_o^{\text{lns},c}(k)$ indicate the number of leaving vehicles without stop).

The acceleration of arriving vehicles is given by

$$a_o^{\text{a},c}(k) = \frac{v_o^{\text{idl},c}(k+1) - v_o^{\text{on},c}(k)}{T} \quad (22)$$

where $v_o^{\text{on},c}(k)$ is the speed of vehicles arriving at the origin link o and $v_o^{\text{idl},c}(k)$ is the speed of the vehicles moving within the queue of origin link o .

The acceleration of waiting vehicles is computed as

$$a_o^{\text{w},c}(k) = \frac{v_o^{\text{idl},c}(k+1) - v_o^{\text{idl},c}(k)}{T} \quad (23)$$

The acceleration of leaving vehicles with stop, entering the first section of link m , is obtained as

$$a_o^{\text{ls},c}(k) = \frac{v_{m,1}^c(k+1) - v_o^{\text{idl},c}(k)}{T} \quad (24)$$

while the acceleration of leaving vehicles without stop is given by

$$a_o^{\text{lns},c}(k) = \frac{v_{m,1}^c(k+1) - v_o^{\text{on},c}(k)}{T} \quad (25)$$

”place Fig. 2 about here”

”place Fig. 3 about here”

The number of vehicles that belong to each group is computed depending on the value of the flow $q_o^c(k)$ leaving the origin link o at time step k . In particular, two cases can be distinguished:

1. if $0 \leq q_o^c(k) \leq \frac{l_o^c(k)}{T}$, corresponding to the case in which the vehicles entering the mainstream are less than the vehicles in the queue (see Fig. 2), the number of vehicles of the four groups is given by

$$n_o^{\text{a},c}(k) = T d_o^c(k) \quad (26)$$

$$n_o^{\text{w},c}(k) = l_o^c(k) - T q_o^c(k) \quad (27)$$

$$n_o^{\text{ls},c}(k) = T q_o^c(k) \quad (28)$$

$$n_o^{\text{lns},c}(k) = 0 \quad (29)$$

2. if $\frac{l_o^c(k)}{T} < q_o^c(k) \leq d_o^c(k) + \frac{l_o^c(k)}{T}$, corresponding to the case in which the vehicles entering the mainstream are more than the vehicles in the queue (see Fig. 3), the number of vehicles is obtained as

$$n_o^{\text{a},c}(k) = T d_o^c(k) + l_o^c(k) - T q_o^c(k) \quad (30)$$

$$n_o^{\text{w},c}(k) = 0 \quad (31)$$

$$n_o^{\text{ls},c}(k) = l_o^c(k) \quad (32)$$

$$n_o^{\text{lns},c}(k) = T q_o^c(k) - l_o^c(k) \quad (33)$$

In accordance with the accelerations previously defined, the macroscopic multi-class VERSIT+ emission model is applied by using (17) for each vehicle class c , for each section i of each link m , for each origin link o and for each time step k . Specifically, the coefficients u_h , $h = 0, \dots, 9$, used in (17) are replaced by suitable coefficients properly identified for the multi-class emission model and the variables are replaced as indicated in Table 1, where $y \in \{a, w, ls, lns\}$ and $v_o^{y,c}(k)$ assumes the following values

$$v_o^{y,c}(k) = \begin{cases} v_o^{\text{on},c}(k) & \text{if } y = a \text{ or } y = lns \\ v_o^{\text{idl},c}(k) & \text{if } y = w \text{ or } y = ls \end{cases} \quad (34)$$

”place Table 1 about here”

5. The proposed framework

As already introduced, the proposed control scheme aims at determining a combined ramp metering and routing strategy in a freeway network. In particular, route guidance is actuated through VMSs (located near the freeway bifurcations) to inform the road users about alternative routes. These indications are assumed to be specifically differentiated for the different classes of vehicles. Moreover, ramp metering is applied in order to regulate the access of traffic to the mainstream through traffic signals installed at the on-ramps. Again, the ramp metering strategy is of the multi-class type, i.e. the different classes of vehicles have dedicated lanes and signals.

The layout of the proposed control framework is depicted in Fig. 4. The overall scheme consists of two main components: the *controllers* and the *gains selector*. The *controllers* are of two types, a route guidance controller and a ramp metering controller. The feedback routing controller computes the *predicted travel time differences* and the *predicted total weighted emission differences* provided, respectively, by the multi-class METANET model and by the multi-class VERSIT+ model, described respectively in Section 3 and Section 4. The prediction models are run periodically and are initialised with the current system state. On the basis of this prediction, the routing control action is computed. The feedback ramp metering controller, instead, computes the on-ramp flow on the basis of the measurements obtained from the real system: the ramp metering control action is updated with a sample time equal to T . A detailed description of the two controllers is reported in Section 6.

”place Fig. 4 about here”

Both the controllers are characterised by different parameters, which can be distinguished in *design parameters*, that are properly fixed by traffic managers to implement specific policies, and *controller gains* which are provided by the *gains selector* module depicted in Fig. 4. This block includes a library of traffic scenarios (corresponding to specific traffic states

and demand patterns), each of which has a set of associated controller gains. Such gains are calibrated through a specific optimisation-based procedure which is applied off-line. Moreover, inside the *gains selector*, a classification algorithm periodically chooses, on the basis of the present system state and estimated demands, the most proper scenario and the corresponding controller gains. The controller gains selector is described in detail in Section 7.

6. The route guidance and ramp metering controllers

6.1. The routing control strategy

The routing control strategy consists in informing the users about the preferred link to choose in a bifurcation, on the basis of the present traffic and emission conditions and, also, by predicting the travel times and emissions for each alternative path. This prediction is run periodically and the routing control action is computed with the same sample time. Specifically, let us denote with \mathcal{N}^C the number of time steps of this routing control sample time (which is then equal to $\mathcal{N}^C T$ [s]), so that the prediction is run and the routing control action is computed at any time step \bar{k} multiple of \mathcal{N}^C . This means that the same routing control action is applied between time step \bar{k} and $\bar{k} + \mathcal{N}^C - 1$. The phases of prediction and routing control action computation are described in detail in the following.

Prediction of travel times and traffic emissions

Since the prediction of travel times and traffic emissions is realised in order to compute routing strategies, this prediction only refers to alternative paths starting from bifurcation nodes, i.e. nodes having two exiting freeway links (more than two exiting links are not possible, according to the network structure defined in Section 3). Inspired by the works Karimi et al. (2004) and Cremer (1995), such prediction is carried out considering some virtual test vehicles, which leave the bifurcation node in order to reach their destinations through alternative paths.

Let us consider a generic bifurcation node n , from which it is possible to reach different destinations $j \in \bar{J}_n$, and let us denote with m and m' the two exiting links. For each pair of nodes (n, j) , $n \in N$, $j \in \bar{J}_n$, the most likely paths are gathered in set $Z_{n,j}$. Since the routing suggestion in node n is related to the choice of one of the two freeway links exiting the node, it is possible to gather the different paths connecting node n to destination j in two sets according to the freeway link exiting node n in each path. The two sets are denoted as the set of *primary* and *secondary* paths on the basis of the most common path choices made by the drivers. Specifically, let us denote with $Z_{n,j}^P$ the set of primary paths having m as first freeway link, and with $Z_{n,j}^S$ the set of secondary paths having m' as first freeway link. Of course, $Z_{n,j} = Z_{n,j}^P \cup Z_{n,j}^S$, whereas $Z_{n,j}^P \cap Z_{n,j}^S = \emptyset$. For each pair of nodes (n, j) , a number of virtual vehicles equal to $|Z_{n,j}|$ is introduced for each class of vehicles. Let us denote with $\delta_{n,j}^z$ the distance [km] between the origin node n and the destination node j in path $z \in Z_{n,j}$.

Referring to a generic time step \bar{k} in which the prediction models are run, two quantities are introduced for each virtual vehicle of class $c = 1, \dots, C$ in path $z \in Z_{n,j}$ and for each time step $k \geq \bar{k}$, i.e. the distance covered by the vehicle in the network $s_{n,j}^{z,c}(k)$ and the total weighted emissions $e_{n,j}^{z,c}(k)$. Such quantities are initialised to 0 for $k = \bar{k}$. The prediction is realised assuming that the routing control actions computed at $\bar{k} - \mathcal{N}^C$ are maintained constant for the whole prediction horizon, while the ramp metering control actions are computed with the PI-ALINEA control law described in Subsection 6.2.

In particular, the covered distance $s_{n,j}^{z,c}(k)$ is updated as follows

$$s_{n,j}^{z,c}(k+1) = s_{n,j}^{z,c}(k) + v_{\bar{m},\bar{i}}^c(k) \cdot T \quad (35)$$

where \bar{m} is the freeway link and \bar{i} the section in which the virtual vehicle of class c is located at time step k along path z .

The total weighted emissions $e_{n,j}^{z,c}$ are calculated as

$$e_{n,j}^{z,c}(k+1) = e_{n,j}^{z,c}(k) + T^{\text{sec}} \phi_{\bar{m}}^c [E_{\bar{m},\bar{i}}^{\text{seg},z,c}(k) + E_{\bar{m},\bar{i},\bar{i}+1}^{\text{cross},z,c}(k)] \quad (36)$$

where $E_{\bar{m},\bar{i}}^{\text{seg},z,c}(k)$ and $E_{\bar{m},\bar{i},\bar{i}+1}^{\text{cross},z,c}(k)$ are the emission factors related to the position of the test vehicle at time step k in freeway link \bar{m} and section \bar{i} , and computed as in (17) according to the notation of Table 1. Note that only one of the emission factors $E_{\bar{m},\bar{i}}^{\text{seg},z,c}(k)$ and $E_{\bar{m},\bar{i},\bar{i}+1}^{\text{cross},z,c}(k)$ is used, since the test vehicle between time steps k and $k+1$ can be either inside a section or at the boundary between two subsequent sections. In (36) T^{sec} is the sample time T expressed in seconds, whereas $\phi_{\bar{m}}^c$ is a weight associated with the passage of vehicles of class c in link \bar{m} . This weight is a design parameter used to suitably penalise the transfer of specific vehicles in critical links of the network (e.g. to dissuade the presence of trucks in city centres or close to protected areas).

The previous computations related to each virtual vehicle end when the vehicle itself reaches its destination, i.e. when $s_{n,j}^{z,c}(k) = \delta_{n,j}^z$. Let us define with $\kappa_{n,j}^{z,c}(\bar{k})$ the duration, in terms of number of time steps, of path z from n to j followed by the virtual vehicle of class c which started its route at time step \bar{k} . Hence, $\kappa_{n,j}^{z,c}(\bar{k})T$ represents the *predicted travel time* and $e_{n,j}^{z,c}(\bar{k} + \kappa_{n,j}^{z,c}(\bar{k}))$ indicates the *predicted total weighted emissions* experienced by the virtual vehicle of class c which left n at time step \bar{k} and followed path z until reaching destination j .

The predicted travel time for primary and secondary paths are calculated at time step \bar{k} as the minimum predicted travel time of paths belonging to the sets $Z_{n,j}^P$ and $Z_{n,j}^S$, respectively. The predicted travel time difference at time step \bar{k} is then obtained as

$$\Delta t_{n,j}^c(\bar{k}) = \min_{z \in Z_{n,j}^S} \{ \kappa_{n,j}^{z,c}(\bar{k})T \} - \min_{z \in Z_{n,j}^P} \{ \kappa_{n,j}^{z,c}(\bar{k})T \} \quad (37)$$

Analogously, the predicted total weighted emission difference is given by

$$\Delta e_{n,j}^c(\bar{k}) = \min_{z \in Z_{n,j}^S} \{ e_{n,j}^{z,c}(\bar{k} + \kappa_{n,j}^{z,c}(\bar{k})) \} - \min_{z \in Z_{n,j}^P} \{ e_{n,j}^{z,c}(\bar{k} + \kappa_{n,j}^{z,c}(\bar{k})) \} \quad (38)$$

Computation of the routing control action

The conditions of Dynamic User Equilibrium have been widely used in route guidance control schemes. These conditions consider that traffic flows with the same origin and destination are distributed in the network so that the travel times on these routes are the same. Moreover, the Dynamic User Equilibrium takes into account the dynamic nature of the traffic conditions, considering that travel times vary over time and space and depend on the level of congestion in the system Peeta and Ziliaskopoulos. (2001); Friesz. (2010). Analogously to the travel time, it is possible to assume that also the level of pollutant emissions depends on time, space and traffic congestion. Based on these considerations, we propose a new eco-routing model named Dynamic Emission Equilibrium, aimed at balancing the weighted pollutant emissions along the suggested routes.

At a generic time step \bar{k} at which the routing control action at node n is computed, the conditions of *Dynamic User Equilibrium* relate the predicted travel time difference with the splitting rates (that we denote with apex ‘t’, since they are referred to travel times), i.e.

$$\Delta t_{n,j}^c(\bar{k}) > 0 \quad \Rightarrow \quad \beta_{m,n,j}^{t,c}(\bar{k}) = 1 \quad (39)$$

$$\Delta t_{n,j}^c(\bar{k}) = 0 \quad \Rightarrow \quad 0 < \beta_{m,n,j}^{t,c}(\bar{k}) < 1 \quad (40)$$

$$\Delta t_{n,j}^c(\bar{k}) < 0 \quad \Rightarrow \quad \beta_{m,n,j}^{t,c}(\bar{k}) = 0 \quad (41)$$

Analogously, the conditions of *Dynamic Emission Equilibrium* may be formulated as a relation between the predicted total weighted emission difference and the splitting rates (denoted in this case with the apex ‘e’ indicating emissions), i.e.

$$\Delta e_{n,j}^c(\bar{k}) > 0 \quad \Rightarrow \quad \beta_{m,n,j}^{e,c}(\bar{k}) = 1 \quad (42)$$

$$\Delta e_{n,j}^c(\bar{k}) = 0 \quad \Rightarrow \quad 0 < \beta_{m,n,j}^{e,c}(\bar{k}) < 1 \quad (43)$$

$$\Delta e_{n,j}^c(\bar{k}) < 0 \quad \Rightarrow \quad \beta_{m,n,j}^{e,c}(\bar{k}) = 0 \quad (44)$$

Note that, in the previous conditions (39)-(41) and (42)-(44), only the splitting rates associated with the choice of link m have been defined, since those for link m' can be easily computed as $\beta_{m',n,j}^{t,c}(\bar{k}) = 1 - \beta_{m,n,j}^{t,c}(\bar{k})$ and $\beta_{m',n,j}^{e,c}(\bar{k}) = 1 - \beta_{m,n,j}^{e,c}(\bar{k})$, $c = 1, \dots, C$, $n = 1, \dots, N$, $j \in \bar{J}_n$.

The proposed feedback routing control strategy is based on PI-controllers, i.e. feedback controllers of the proportional-integral type. Let us consider the two PI-controllers adopted at time step \bar{k} to define the splitting rates $\beta_{m,n,j}^{t,c}(\bar{k})$ and $\beta_{m,n,j}^{e,c}(\bar{k})$. Taking into account conditions (39)-(41) and (42)-(44), such controllers are defined as follows

$$\beta_{m,n,j}^{t,c}(\bar{k}) = \beta_{m,n,j}^{t,c}(\bar{k}-1) + K_P^{t,c}[\Delta t_{n,j}^c(\bar{k}) - \Delta t_{n,j}^c(\bar{k}-1)] + K_I^{t,c} \Delta t_{n,j}^c(\bar{k}) \quad (45)$$

$$\beta_{m,n,j}^{e,c}(\bar{k}) = \beta_{m,n,j}^{e,c}(\bar{k}-1) + K_P^{e,c}[\Delta e_{n,j}^c(\bar{k}) - \Delta e_{n,j}^c(\bar{k}-1)] + K_I^{e,c} \Delta e_{n,j}^c(\bar{k}) \quad (46)$$

$c = 1, \dots, C$, $n = 1, \dots, N$, $j \in \bar{J}_n$, where $K_P^{t,c}$, $K_I^{t,c}$, $K_P^{e,c}$ and $K_I^{e,c}$, $c = 1, \dots, C$, are the gain parameters of the PI-controllers. It is worth noting that the resulting splitting rates $\beta_{m,n,j}^{t,c}(\bar{k})$ and $\beta_{m,n,j}^{e,c}(\bar{k})$ should be truncated to the admissible interval $[0, 1]$.

The splitting rates which jointly consider the effect of both assignment conditions are given by the following weighted sum:

$$\beta_{m,n,j}^{C,c}(\bar{k}) = \alpha^c \cdot \beta_{m,n,j}^{t,c}(\bar{k}) + (1 - \alpha^c) \cdot \beta_{m,n,j}^{e,c}(\bar{k}) \quad (47)$$

where α^c are design parameters defined for class $c = 1, \dots, C$, with $0 \leq \alpha^c \leq 1$. Parameters α^c , $c = 1, \dots, C$, are fixed in order to apply specific control policies for each vehicle class, by properly balancing travel times and total weighted emissions.

Since the routing controller is of the predictive type, its performance can be decreased in case of model mismatch. As highlighted in Wang et al. (2002), such a mismatch can be caused by several reasons, e.g. inaccuracy of the prediction model, of the model parameter estimates, of the state measurements, and so on. In these cases, the control scheme should be enriched with outer feedback loops in order to reject the model mismatch. For instance, in Wang et al. (2002) the model mismatch caused by unknown compliance rates is dealt with by introducing an outer feedback loop which updates the splitting rates to be actuated in the freeway network on the basis of those computed by the predictive feedback rule and by taking into account measured travel time differences. Such a scheme could be extended to the present case, by taking into account not only the experienced travel time differences but also the measured emission differences, distinguished per vehicle class.

6.2. The ramp metering control strategy

The ramp metering control strategy is based on feedback controllers of the proportional-integral type as well, and in particular on the multi-class PI-ALINEA (see Pasquale et al. (2014) for major details). As aforementioned, the control sample time interval of the ramp metering strategy is equal to T .

Let us first of all introduce the variable $f_o^c(k)$ indicating the ratio, at time step k , of the number of vehicles of class $c = 1, \dots, C$ over the entire number of vehicles, which are present in origin link $o = 1, \dots, O$ and in the mainstream section immediately downstream link o (namely the first section of the downstream leaving link m). Such quantity can be computed as

$$f_o^c(k) = \frac{\eta^c \cdot [\rho_{m,1}^c(k)L_m + l_o^c(k)]}{\sum_{c=1}^C \eta^c \cdot [\rho_{m,1}^c(k)L_m + l_o^c(k)]} \quad (48)$$

Referring to a generic origin link o that is a controlled on-ramp, the flow of class $c = 1, \dots, C$ that should enter at time step k is computed as follows

$$\bar{q}_o^c(k) = \max \left\{ q_o^{\min,c}, q_o^c(k-1) - K_P^c \cdot [\rho_{m,1}^c(k-1) - \rho_{m,1}^c(k-2)] \right. \\ \left. + K_R^c \cdot f_o^c(k-1)[\hat{\rho}_{m,1} - \rho_{m,1}(k-1)] \right\} \quad (49)$$

where $\hat{\rho}_{m,1}$ is the total density set-point of the first section of link m , K_P^c and K_R^c are gain parameters of the regulator, whereas $q_o^{\min,c}$ is the minimum traffic volume for class c and origin link o . A possible choice is to fix the total density set-point equal to the critical density, i.e. $\hat{\rho}_{m,1} = \rho_{m,1}^{\text{cr}}$. Note that, when in real cases the measurements are provided in terms of occupancy instead of density, the previous relations can be applied by mapping the occupancy measurements to a density scale.

7. The controller gains selector

As mentioned before, the parameters of the proposed controllers can be gathered in two sets depending on their characteristics. The first set, denoted by $\mathbb{W} = \{\alpha^c, \phi_m^c, \hat{\rho}_m, \mathcal{N}^C, c = 1, \dots, C, m = 1, \dots, M\}$, gathers all the design parameters which are used to implement specific traffic policies. These parameters are fixed following the indications of freeway managers.

The second set, denoted by $\mathbb{K} = \{K_P^{t,c}, K_I^{t,c}, K_P^{e,c}, K_I^{e,c}, K_P^c, K_R^c, c = 1, \dots, C\}$, collects the controller gains. Let us now describe the selection procedure of the controller gains.

First of all, a finite set Ξ of traffic scenarios is defined to take into account different traffic conditions. Each scenario $\sigma \in \Xi$ is characterised by a set of initial traffic conditions and a demand pattern. Each scenario $\sigma \in \Xi$ is associated with a set \mathbb{K}^σ of controller gains. The controller gains to be used by the controllers are chosen with a given sampling time T^S [s], normally larger than T . This means that every T^S seconds the selector identifies the most adequate scenario $\bar{\sigma}$ for representing the present traffic conditions. This can be done by using classification techniques or clustering methods D.Michie et al. (1994); Alpaydin. (2009); Everitt et al. (2011); Aggarwal. (2014); Hennig et al. (2015). On the basis of the chosen scenario $\bar{\sigma}$, the selector module feeds the controllers with the corresponding set $\mathbb{K}^{\bar{\sigma}}$ of gains.

The controller gains associated with each scenario are found by off-line running an optimisation-based procedure, whose details are reported in the following subsection.

7.1. Optimisation-based calibration of the controller gains

The controller gains gathered in set \mathbb{K}^σ are found by solving an optimisation problem in which the minimisation of travel times and the minimisation of traffic emissions are explicitly taken into account. The first

objective is the Total Time Spent by vehicles in the network, denoted with TTS [PCE·h]. With reference to a time horizon of H time steps, the TTS in the multi-class case can be computed as

$$TTS = \sum_{k=0}^{H-1} T \left[\sum_{m=1}^M \sum_{i=1}^{N_m} L_m \sum_{c=1}^C \eta^c \rho_{m,i}^c(k) + \sum_{o=1}^O \sum_{c=1}^C \eta^c l_o^c(k) \right] \quad (50)$$

The second objective is TE [g], i.e. the Total Emissions in the freeway links and in the origin links, which can be computed as

$$TE = \sum_{k=0}^{H-1} \sum_{c=1}^C T^{\text{sec}} \left[\sum_{m=1}^M \left(\sum_{i=1}^{N_m} E_{m,i}^{\text{seg},c}(k) + \sum_{i=1}^{N_m-1} E_{m,i,i+1}^{\text{cross},c}(k) \right) + \sum_{o=1}^O \sum_{y \in \{\text{a,w,ls,lns}\}} E_o^{\text{orig},y,c}(k) \right] \quad (51)$$

The general formulation of the optimisation problem for the calibration of controller gains is the following.

Problem 1. *Given the system initial conditions $\rho_{m,i,j}^c(0)$, $v_{m,i}^c(0)$, $c = 1, \dots, C$, $m = 1, \dots, M$, $i = 1, \dots, N_m$, $j = 1, \dots, J_m$, $l_{o,j}^c(0)$, $c = 1, \dots, C$, $o = 1, \dots, O$, $j = 1, \dots, \bar{J}_o$, the estimated demands $d_{o,j}^c(k)$, $\theta_{o,j}^c(k)$, $c = 1, \dots, C$, $o = 1, \dots, O$, $j = 1, \dots, \bar{J}_o$, $k = 0, \dots, H-1$, the initial values $\beta_{m,n,j}^{\text{t},c}(0)$ and $\beta_{m,n,j}^{\text{e},c}(0)$, the predicted differences $\Delta t_{n,j}^c(\bar{k})$, $\Delta t_{n,j}^c(\bar{k}-1)$, $\Delta e_{n,j}^c(\bar{k})$, $\Delta e_{n,j}^c(\bar{k}-1)$, $\bar{k} = h\mathcal{N}^C$, $h = 1, \dots, H/\mathcal{N}^C - 1$, find the set \mathbb{K}^σ of positive controller gains that minimises*

$$\mathcal{J} = \omega \cdot \Gamma \cdot TE + (1 - \omega) \cdot TTS \quad (52)$$

subject to (1), (2), (9), (12)-(15), (17) with Table 1, (45)-(47), (49).

In Problem 1, the two performance indices TTS and TE are reported to the same order of magnitude thanks to coefficient Γ and are arbitrarily weighted by $\omega \in [0, 1]$. Problem 1 is a nonlinear optimisation problem that can be solved by both gradient-based nonlinear solvers and gradient-free techniques Ruszczynski. (2006); Pham et al. (2011); Rios and Sahinidis. (2013). In many cases, nonlinear problems arising in traffic control have been solved efficiently by applying multi-start methods Burger et al. (2013).

8. Simulation results

A specific case study of a freeway network is tested via simulation by considering the implementation of several control policies. These tests aim, firstly, to assess the effectiveness of the proposed methodology, and, secondly, to verify the flexibility of the proposed controller to implement specific policies for the different classes of vehicles, as well as to privilege or penalise specific freeway links or paths. The simulation results obtained

from this analysis, and proposed in this section, have been achieved by adopting the multi-class METANET model and the macroscopic VER-SIT+ model to reproduce the traffic behaviour and to compute CO₂ emissions of the freeway network; such models are also utilised to estimate the travel times and the CO₂ emissions along the selected paths in the prediction models used by the routing controller. In this analysis two types of vehicles, namely cars and trucks, have been taken into account distinguishing specific control actions for each of them.

8.1. Description of the case study

The freeway network considered to test the combined ramp metering and routing strategy is shown in Fig. 5. It is composed of twelve freeway links, named m_1 to m_{12} , each one with sections 800 [m] long and three lanes, of four origin links o_1 to o_4 , and two destinations D1 and D2. If the multi-class control strategy is applied, the origin links o_2 , o_3 , o_4 are controlled via ramp metering, whereas VMSs are placed to bifurcations located at nodes n_3 and n_8 in order to display route guidance indications. Specifically, node n_3 is connected with destination D1 by only one primary path belonging to $Z_{n_3,D1}^P$, composed of the freeway links m_3 – m_4 – m_5 – m_{10} , with a total length of 12 [km], and by only one secondary path belonging to $Z_{n_3,D1}^S$, constituted by the freeway links m_6 – m_7 – m_8 – m_5 – m_{10} , with a total length of 16.8 [km]. From node n_3 it is also possible to reach destination D2 by means of two primary paths belonging to set $Z_{n_3,D2}^P$, i.e. m_6 – m_7 – m_9 – m_{12} (11.2 [km]) and m_6 – m_7 – m_8 – m_5 – m_{11} – m_{12} (14.4 [km]), and one secondary path belonging to $Z_{n_3,D2}^S$ given by the freeway links m_3 – m_4 – m_5 – m_{11} – m_{12} , with a total length of 14.4 [km]. Only one path connects node n_8 with destination D1, i.e. m_8 – m_5 – m_{10} , while two alternative paths may be adopted to reach destination D2 from node n_8 , with $Z_{n_8,D2}^P$ composed of path m_9 – m_{12} , with a total length of 3.2 [km], and $Z_{n_8,D2}^S$ composed of path m_8 – m_5 – m_{11} – m_{12} , with an overall length of 11.2 [km].

”place Fig. 5 about here”

For the present case study, the splitting rates at node n_3 without route recommendations are fixed as follows: $\beta_{m_3,n_3,D1}^{N,c}(k) = 1$, $\beta_{m_3,n_3,D2}^{N,c}(k) = 0.55$, and consequently $\beta_{m_6,n_3,D1}^{N,c}(k) = 0$ and $\beta_{m_6,n_3,D2}^{N,c}(k) = 0.45$, $c = 1, 2$, $k = 0, \dots, K - 1$. The splitting rates without route recommendations at node n_8 are $\beta_{m_8,n_8,D2}^{N,1}(k) = 0.1$, $\beta_{m_8,n_8,D2}^{N,2}(k) = 0.2$, $\beta_{m_9,n_8,D2}^{N,1}(k) = 0.9$, $\beta_{m_9,n_8,D2}^{N,2}(k) = 0.8$, $k = 0, \dots, K - 1$. In presence of routing control actions, the splitting rates are computed by means of the routing controller presented in Section 6 and considering a complete compliance with the route recommendations.

”place Fig. 6 about here”

For the simulation analysis, the sample time is $T^{\text{sec}} = 10$ [s] and a total time horizon of 3 [h] is considered, corresponding to $K = 1080$. A

constant demand is considered at the origin link o_1 for the whole time horizon, whereas at the origin links o_2, o_3, o_4 trapezoidal demand profiles for both vehicle classes are assumed, as shown in Fig. 6. Given the network configuration, from all the origin links it is possible to reach the two destinations, and it is assumed that 50% of the traffic demand in these links is destined to D1, while the remaining 50% has D2 as destination. The following traffic model parameters are selected: $v_{m,i}^{f,1} = 120$ [km/h], $v_{m,i}^{f,2} = 90$ [km/h], $\rho_{m,i}^{\max} = 200$ [PCE/km/lane], $\rho_{m,i}^{\text{cr}} = 46.66$ [PCE/km/lane], $\forall m, \forall i$. The conversion factors are $\eta^1 = 1$ and $\eta^2 = 4$. As for the VERSIT+ emission model, the origin link speed is considered constant and set equal to 30 [km/h] for both vehicle classes, and the speed of the vehicles moving within the queue, considered constant as well, is set equal to 5 [km/h] for the two classes.

Fig. 7 shows the profiles of the density in the freeway links in the uncontrolled case. It is possible to observe that the congestion appears first on the downstream link of the origin link o_2 , and then worsens in the links m_3, m_4 , and m_5 due to incoming flows from the links o_3 and m_8 since, in absence of route recommendations, most of the vehicles choose these links to reach destinations D1 and D2. The congestion dissolves in the links m_{10} and m_{11} , since the flow coming from node n_6 is split between these two links. Moreover, it is possible to observe that the congestion on links m_2 and m_4 has a slight influence on links m_1 and m_8 , while links m_6, m_7, m_9 and m_{12} are completely uncongested. A different trend is observed in Fig. 8, which shows the CO₂ emissions profiles in the freeway links, where the highest CO₂ emissions are in the freeway links m_1, m_2, m_3, m_4 , and m_5 and a rather high concentration of emissions is present also in the links m_6, m_9 and m_{11} , due to the higher speeds observed in these stretches. In this case, the Total Time Spent is equal to 9002 [PCE·h], whereas the Total Emissions are 129316 [kg].

”place Fig. 7 about here”

”place Fig. 8 about here”

8.2. Performance evaluation of the controller

In order to evaluate the performance of the proposed methodology, five control policies have been implemented. All these cases have in common the features of the traffic scenario previously described, and the controller gains found by solving Problem 1. In particular, the calibration of the controller gains has been performed adopting the Simulated Annealing algorithm. Simulated Annealing is one of the most used iterative stochastic algorithms for global nonlinear optimisation since it is easy to implement, robust and applicable to a wide class of global optimisation problems. An important characteristic of Simulated Annealing algorithms is the procedure for the cooling schedule, i.e. the update of the temperature parameter. The Simulated Annealing algorithm adopted

in this work presents specific features of the cooling schedule, as done in Anghinolfi et al. (2016). The effectiveness of this algorithm in the field of traffic control has been verified in Pasquale et al. (2016a), where it is compared with other derivative-free algorithms.

The results of such optimisation are reported in Table 2, where the values of all the controller gains of set \mathbb{K} are shown. As for the design parameters of the controller in \mathbb{W} , \mathcal{N}^C has been set equal to 30, corresponding to a routing control sample time of 5 [min], whereas the value of the density set point $\hat{\rho}_{m,1}$ has been chosen equal to the critical density, $\forall m$. Moreover, each case is characterised by different values of the design parameters ϕ_m^c , α^c , $c = 1, 2$, $m = 3, 4$, as shown in Table 3. Note that, in all cases, $\phi_m^c = 1$, $c = 1, 2$, $m \neq 3, 4$. Table 3 also reports, for each case, the percentage reduction of the total time spent R_{TTS} and of the total emissions R_{TE} , compared with the uncontrolled case.

”place Table 2 about here”

”place Table 3 about here”

Let us start by describing the results obtained in Case 1, where $\phi_m^c = 1$, $c = 1, 2$, $m = 3, 4$, and $\alpha^1 = \alpha^2 = 0.5$ in order to balance, in the same way, the emissions and the travel times for all the considered paths. Observing Fig. 9, in which the values of the splitting rates at node n_3 are shown, it may be stated that the use of link m_3 to reach destination D1 remains favourable for cars, while trucks, that have lower speeds and produce higher emissions, are largely directed to the alternative path. Differently, for both classes of vehicles, the controller mainly suggests the path connected to link m_6 in order to reach destination D2. Fig. 10, instead, shows the splitting rates related to node n_8 : it is possible to observe that the controller mainly acts on trucks, which are redirected to link m_8 in order to reach destination D2. Finally, Fig. 11 shows the queue lengths and the entering flows for the 3 controlled origin links: only at the origin link o_2 both cars and trucks are queued (corresponding to a reduction of the entering flow compared with the demand), since the effects of the routing strategy do not require the activation of the ramp metering at links o_3 and o_4 . Note that the application of this control strategy implies a TTS reduction equal to 25.85% and a TE reduction of 27.10% compared with the uncontrolled case, as reported in Table 3.

”place Fig. 9 about here”

”place Fig. 10 about here”

”place Fig. 11 about here”

In Case 2, only the emissions along the possible routes have been balanced, which corresponds to set $\alpha^1 = \alpha^2 = 0$. In this case, the routing controller for node n_3 suggests, both to cars and trucks, to use link m_3 to reach destination D1, while, for most of the simulated time, cars and

trucks are directed to link m_6 to reach destination D2, as shown in Fig. 12. With regard to the trajectory of the control variables at node n_8 and depicted in Fig. 13, no particular deviations are observed compared to the no-control case, since in this solution the total volume of vehicles directed towards link m_6 is lower than the one observed in Case 1. Finally, the actions carried out by ramp metering are very similar to the ones performed in Case 1.

”place Fig. 12 about here”

”place Fig. 13 about here”

In Case 3, instead, choosing $\alpha^c = 1$, $c = 1, 2$, the implemented control strategy aims at equalising only the travel times along the possible paths. To this end, the routing controller gradually splits the vehicles toward link m_6 in order to reach destination D2, while only trucks are redirected to link m_6 to reach destination D1 (Fig. 14). Fig. 15 shows the control variables related to node n_8 , where, to alleviate the congestion, trucks are gradually deviated to link m_8 . Also in this case, the ramp metering control is activated only at origin link o_2 .

”place Fig. 14 about here”

”place Fig. 15 about here”

In the last two cases analysed in this section, the design parameters $\phi_m^c \geq 1$, $c = 1, 2$, $m = 3, 4$, are introduced to penalise the transit of the vehicles in specific freeway links of the network. Specifically, in Case 4 the travel of trucks in links m_3 and m_4 is discouraged increasing the evaluation of the emissions in these stretches with a factor 2.5, while α^c is set equal to 0.5 for both vehicle classes. Observing Fig. 16, it is possible to state that almost all the trucks are encouraged to use link m_6 to reach destinations D1 and D2, such as most of the cars are deviated to link m_6 in order to reach D2. Instead, Fig. 17 shows that, after half an hour of simulation, 50% of the trucks uses the alternative path that connects node n_8 with destination D2. Also for this case the ramp metering is activated only at origin link o_2 . Adopting this solution, the total emissions on path m_3 - m_4 - m_5 - m_{10} (i.e. the one specifically discouraged by the adopted policy) are reduced to 29232 [kg] compared with 70537 [kg] produced in the uncontrolled case (that corresponds to a reduction of 58.56%) and with 30609 [kg] resulting for the adoption of the control strategy proposed in Case 1 (i.e. 4.5% reduction).

”place Fig. 16 about here”

”place Fig. 17 about here”

Finally, in the last case proposed in this section, i.e. Case 5, the transit of both cars and trucks in links m_3 and m_4 is penalised adopting the parameters indicated in Table 3. With this configuration the flows of ve-

hicles are mainly directed to link m_6 to reach destination D1, while link m_6 , after half an hour of simulation, is rather completely utilised by cars and trucks to arrive at destination D2 (see Fig. 18). The splitting rates at node n_8 (shown in Fig. 19) indicate a quite similar behaviour compared with Case 4. This flow increase in link m_6 involves the activation of the ramp metering strategies even in link o_4 , as depicted in Fig. 20. As shown in Table 3, the application of this strategy involves the lowest global improvements in terms of total time spent and total emissions; however, it is worth noting that in this case the emissions in the path m_3 – m_4 – m_5 – m_{10} are reduced to 21681 [kg], which corresponds to a 69% reduction compared with the uncontrolled case, and a 29% reduction compared with Case 1.

”place Fig. 18 about here”

”place Fig. 19 about here”

”place Fig. 20 about here”

The reported results show the efficacy of the proposed control scheme in reducing both the performance indices, i.e. total time spent and total emissions, in all the cases presented in this section. Such a control scheme allows different degrees of freedom in managing a freeway network: separate control actions can be dedicated to different vehicle classes, it is possible to privilege one of the two performance indices and, also, priorities (or penalties) can be associated with specific paths. Hence, besides being very effective in regulating traffic flow, the proposed controller presents a high flexibility in implementing specific control policies.

9. Conclusions

A multi-class combined ramp metering and routing control strategy has been proposed in the paper with the aim of reducing, in a balanced way, the total travel time and the total emissions in freeway traffic networks. The proposed controller is of the predictive and feedback type, i.e. the control action depends on the measured system state and on predictions of the system evolution. These predictions are realised exploiting the multi-class METANET model, to account for the traffic dynamics in the network, and the multi-class macroscopic VERSIT+ model, to compute the emissions in the whole freeway network. The controller is based on several parameters, some of which are design parameters to be fixed according to the policies which are to be implemented, while some others are controller gains, which are calibrated with an optimisation-based procedure described in the paper. The presented simulation results show significant improvements of the freeway network performance, in terms of reduction of the total time spent and reduction of the total emissions, in case the proposed control strategy is applied. Besides, it is worth observing that the controller is quite flexible and is able to pursue specific objectives, such as the reduction of the emissions on specific links, or to give different priorities to different classes of vehicles.

To conclude, the proposed approach meets the design requirements established at the beginning of this work, even though it would be worth to further investigate some aspects. The adoption of system optimum concepts (instead of the user equilibrium logic followed in the paper) could lead to different control actions to be compared with the present ones. Different prediction methods could be analysed to compute the predicted travel times and emissions on which the routing actions are based. Finally, an MPC scheme for jointly minimising travel times and traffic emissions could be defined, but this would require also the definition of efficient solution algorithms in order to preserve the practical applicability of the control scheme.

References

- Aggarwal, C., 2014. *Data Classification: Algorithms and Applications*.
- Ahn, K., Rakha, H., 2008. The effects of route choice decisions on vehicle energy consumption and emissions. *Transportation Research Part D* 13, 151–167.
- Ahn, K., Rakha, H., Trani, A., Aerde, M.V., 2002. Estimating vehicle fuel consumption and emissions based on instantaneous speed and acceleration levels. *Journal of Transportation Engineering* 128, 182–190.
- Alpaydin, E., 2009. *Introduction to Machine Learning*.
- Anghinolfi, D., Canepa, E., Cattanei, A., Paolucci, M., 2016. Psychoacoustic optimization of the spacing of propellers, helicopter rotors and axial fans. *Journal of Propulsion and Power* 32, 1422–1432.
- Bachman, W., Sarasua, W., Hallmark, S., Guensler, R., 2000. Modeling regional mobile source emissions in a geographic information system framework. *Transportation Research Part C* 8, 205–229.
- Bagnerini, P., Rasche, M., 2003. A multiclass homogenized hyperbolic model of traffic flow. *SIAM Journal on Mathematical Analysis*. 35, 949–973.
- Bellemans, T., De Schutter, B., De Moor, B., 2006. Model predictive control for ramp metering of motorway traffic: A case study. *Control Engineering Practice* 14, 757–767.
- Ben-Akiva, M., Bottom, J., Ramming, M., 2001. Route guidance and information systems. *Journal of Systems and Control Engineering* 215, 317–324.
- Burger, M., Van Den Berg, M., Hegyi, A., De Schutter, B., Hellendoorn, J., 2013. Considerations for model-based traffic control. *Transportation Research Part C* 35, 1–19.
- Burley, M., Gaffney, J., 2013. *Managed freeways freeway ramp signals handbook*. Technical Report. VicRoads.

- Caligaris, C., Sacone, S., Siri, S., 2007. Optimal ramp metering and variable speed signs for multiclass freeway traffic, in: Proc. of the European Control Conference, pp. 1780–1785.
- Caligaris, C., Sacone, S., Siri, S., 2010. On the Payne-Whitham differential model stability constraints in one-class and two-class cases. *Applied Mathematical Sciences* , 3795–3821.
- Cremer, M., 1995. On the calculation of individual travel times by macroscopic models, in: Proc. of the 6th International Vehicle Navigation and Information Systems Conference, pp. 187–193.
- Csikós, A., Varga, I., Hangos, K., 2015. Modeling of the dispersion of motorway traffic emission for control purposes. *Transportation Research Part C* 58, 598–616.
- Daganzo, C., 1997. A continuum theory of traffic dynamics for freeways with special lanes. *Transportation Research Part B* 31, 83–102.
- Deo, P., De Schutter, B., Hegyi, A., 2009. Model predictive control for multi-class traffic flows, in: Proc. of the 12th IFAC Symposium on Transportation Systems, pp. 25–30.
- D.Michie, Spiegelhalter, D., Taylor, C., 1994. *Machine Learning, Neural and Statistical Classification*.
- Everitt, B., Landau, S., Leese, M., Stahl, D., 2011. *Cluster Analysis*.
- Ferrara, A., Nai Oleari, A., S.Sacone, Siri, S., . Freeways as systems of systems: a distributed model predictive control scheme. *IEEE Systems Journal* .
- Ferrara, A., Sacone, S., Siri, S., 2015. Event-triggered model predictive schemes for freeway traffic control. *Transportation Research C* 58, 554–567.
- Friesz, T., 2010. Dynamic user equilibrium., in: *Dynamic Optimization and Differential Games*, Chapter 9., Springer, pp. 411–456.
- Gomes, G., Horowitz, R., 2006. Optimal freeway ramp metering using the asymmetric cell transmission model. *Transportation Research Part C* 14, 244–262.
- Hausberger, S., Rexeis, M., Zallinger, M., Luz, R., 2009. Emission factors from the model PHEM for the HBEFA Version 3. Technical Report. Report Nr. I-20/2009 Haus-Em, Graz University of Technology.
- Hegyi, A., Bellemans, T., De Schutter, B., 2009. Freeway traffic management and control, in: *Encyclopedia of Complexity and Systems Science*. Springer, pp. 3943–3964.
- Henn, V., 2000. Fuzzy route choice model for traffic assignment. *Fuzzy Sets and Systems* 116, 77–101.

- Hennig, C., Meila, M., Murtagh, F., Rocci, R., 2015. Handbook of Cluster Analysis.
- Holland, E., Woods, A., 1997. A continuum model for the dispersion of traffic on two-lane roads. *Transportation Research Part B* 31, 473–485.
- Hoogendoorn, S., Bovy, P., 2000. Continuum modeling of multiclass traffic flow. *Transportation Research Part B* 34, 123–146.
- Hoogendoorn, S., Bovy, P., 2001. Platoon-based multiclass modeling of multilane traffic flow. *Networks and Spatial Economics* 1, 137–166.
- Joumard, R., André, J., Rapone, M., Zallinger, M., Kljun, N., Andre, M., Samaras, Z., Roujol, S., Laurikko, J., et al., M.W., 2007. Emission factor modelling and database for light vehicles. Technical Report. Artemis deliverable, Report n. LTE 0523.
- Karimi, A., Hegyi, A., De Schutter, B., Hellendoorn, H., Middelham, F., 2004. Integration of dynamic route guidance and freeway ramp metering using model predictive control, in: *Proc. of the American Control Conference*, pp. 5533–5538.
- Kaufman, D., Nonis, J., Smith, R., 1998. A mixed integer linear programming model for dynamic route guidance. *Transportation Research Part B* 32, 431–440.
- Kotsialos, A., Papageorgiou, M., Mangeas, M., Haj-Salem, H., 2002. Coordinated and integrated control of motorway networks via non-linear optimal control. *Transportation Research Part C* 10, 65–84.
- Ligterink, N.E., De Lange, R., Schoen, E., 2009. Refined vehicle and driving-behavior dependencies in the VERSIT+ emission model, in: *Proc. of the ETAPP Symposium*, pp. 177–186.
- Liu, S., De Schutter, B., Hellendoorn, H., 2013. Multi-class traffic flow and emission control for freeway networks, in: *Proc. of the 16th International IEEE International Conference on Intelligent Transportation Systems*, pp. 2223–2228.
- Liu, S., De Schutter, B., Hellendoorn, H., 2014a. Integrated traffic flow and emission control based on FASTLANE and the multi-class VT-macro model, in: *Proc. of the 2014 European Control Conference*, pp. 2908–2913.
- Liu, S., De Schutter, B., Hellendoorn, H., 2014b. Model predictive traffic control based on a new multi-class METANET model, in: *Proc. of the 19th IFAC World Congress*, pp. 8781–8785.
- Liu, S., Hellendoorn, H., De Schutter, B., 2017. Model predictive control for freeway networks based on multi-class traffic flow and emission models. *IEEE Transactions on Intelligent Transportation Systems* 18, 306–320.
- Logghe, S., Immers, L., 2008. Multi-class kinematic wave theory of traffic flow. *Transportation Research Part B* 42, 523–541.

- Luo, L., Ge, Y.E., Zhang, F., X.Ban., 2016. Real-time route diversion control in a model predictive control framework with multiple objectives: Traffic efficiency, emission reduction and fuel economy. *Transportation Research Part D* 48, 332–356.
- Muralidharan, A., Horowitz., R., 2015. Computationally efficient model predictive control of freeway networks. *Transportation Research Part C* 58, 532–553.
- National Research Council, 1994. *Highway Capacity Manual*. Technical Report. Transportation Research Board: special report 209, Washington, DC.
- Negrenti, E., 1999. The 'corrected average speed' approach in ENEA's TEE model: an innovative solution for the evaluation of the energetic and environmental impacts of urban transport policies. *Science of the total environment* 235, 411–413.
- New Zeland Transport Agency, 2011. ITS specification - Ramp meter site layout. Technical Report.
- Ntziachristos, L., Kouridis., C., 2007. Road transport emission chapter of the EMEP/CORINAIR Emission Inventory Guidebook. Technical Report 16. European Environment Agency Technical Report.
- Ntziachristos, L., Samaras, Z., Eggleston, S., Gorißen, N., Hassel, D., et al., A.H., 2000. COPERT III. Technical Report. Computer programme to calculate emissions from road transport, methodology and emission factors (version 2.1), European Energy Agency (EEA), Copenhagen.
- Pang, G., Takabashi, K., Yokota, T., Takenaga., H., 1999. Adaptive route selection for dynamic route guidance system based on fuzzy-neural approaches. *IEEE Transactions on Vehicular Technology* 48, 2028–2041.
- Papageorgiou, M., Blosseville, J., Salem., H., 1990. Modelling and real-time control of traffic flow on the southern part of Boulevard Périphérique in Paris: Part I: Modelling. *Transportation Research Part A* 24, 345–359.
- Papageorgiou, M., Diakaki, C., Dinopoulou, V., Kotsialos, A., Wang., Y., 2003. Review of road traffic control strategies, in: *Proc. of the IEEE*, pp. 2043–2067.
- Papageorgiou, M., Hadj-Salem, H., Blosseville., J.M., 1991. ALINEA: A local feedback control law for on-ramp metering. *Transportation Research Record* , 58–64.
- Papageorgiou, M., Kotsialos., A., 2002. Freeway ramp metering: an overview. *IEEE Transactions on Intelligent Transportation Systems* 3, 271–281.
- Papageorgiou, M., Kotsialos., A., 2004. Nonlinear optimal control applied to coordinated ramp metering. *IEEE Transactions on Control Systems Technology* 12, 920–933.

- Papageorgiou, M., Papamichail, I., 2008. Overview of traffic signal operation policies for ramp metering. *Transportation Research Record* 2047, 28–36.
- Papamichail, I., Papageorgiou, M., Wang, Y., 2007. Motorway traffic surveillance and control. *European Journal of Control* 13, 297–319.
- Pasquale, C., Anghinolfi, D., Sacone, S., Siri, S., Papageorgiou, M., 2016a. A comparative analysis of solution algorithms for nonlinear freeway traffic control problems., in: *Proc. of the 19th IEEE International Conference on Intelligent Transportation Systems*, pp. 1773–1778.
- Pasquale, C., Liu, S., Siri, S., Sacone, S., De Schutter, B., 2015a. A new emission model including on-ramps for two-class freeway traffic control, in: *Proc. of the 18th IEEE International International Conference on Intelligent Transportation Systems*, pp. 1143–1149.
- Pasquale, C., Papamichail, I., Roncoli, C., Sacone, S., Siri, S., Papageorgiou, M., 2015b. Two-class freeway traffic regulation to reduce congestion and emissions via nonlinear optimal control. *Transportation Research Part C* 55, 85–99.
- Pasquale, C., Sacone, S., Siri, S., 2014. Two-class emission traffic control for freeway systems, in: *Proc. of the 19th IFAC World Congress*, pp. 936–941.
- Pasquale, C., Siri, S., Sacone, S., De Schutter, B., 2016b. A multi-class ramp metering and routing control scheme to reduce congestion and traffic emissions in freeway networks, in: *Proc. of the 14th IFAC Symposium on Control in Transportation Systems*, pp. 329–334.
- Pavlis, Y., M.Papageorgiou, 1999. Simple decentralized feedback strategies for route guidance in traffic networks. *Transportation Science* 33, 264–278.
- Peeta, S., Ziliaskopoulos, A., 2001. Foundations of dynamic traffic assignment: the past, the present and the future. *Networks and Spatial Economics* 1, 233–265.
- Pham, N., Malinowski, A., Bartczak, T., 2011. Comparative study of derivative free optimization algorithms. *IEEE Transactions on Industrial Informatics* 7, 592–600.
- Pisarski, D., Canudas de Wit, C., 2016. Nash game based distributed control design for balancing of traffic density over freeway networks. *IEEE Transactions on Control of Network Systems* 3, 149–161.
- Rakha, H., Ahn, K., Moran, K., 2012. Integration framework for modeling eco-routing strategies: logic and preliminary results. *International Journal of Transportation Science and Technology* 1, 259–274.
- Richardson, A., et al., R.A., 1981. Fuel consumption models and data needs for the design and evaluation of urban traffic systems, in: *Proc. of the Transportation Conference*, pp. 21–28.

- Rios, L., Sahinidis, N., 2013. Derivative-free optimization: a review of algorithms and comparison of software implementations. *Journal of Global Optimization* 56, 1247–1293.
- Ruszczynski, A., 2006. *Nonlinear Optimization*.
- Sacone, S., Siri, S., 2012. A control scheme for freeway traffic systems based on hybrid automata. *Discrete Event Dynamic Systems: Theory and Applications* 22, 3–25.
- Schreiter, T., Van Lint, H., Hoogendoorn, S., 2011. Multi-class ramp metering: concepts and initial results, in: *Proc. of the 14th IEEE International Conference on Intelligent Transportation Systems*, pp. 885–889.
- Smit, R., Smokers, R., Schoen, E., 2005. VERSIT+ LD: development of a new emission factor model for passenger cars linking real-world emissions to driving cycle characteristics, in: *Proc. of the 14th Symposium on Transport and Air Pollution*, pp. 177–186.
- Spiliopoulou, A., I.Papamichail, Papageorgiou, M., Tyrinopoulos, I., Chrysoulakis, J., 2015. Macroscopic traffic flow model calibration using different optimization algorithms., in: *Proc. of the 4th International Symposium of Transport Simulation*, pp. 144–157.
- Tzeng, G., Chen, C., 1993. Multiobjective decision making for traffic assignment. *IEEE Transactions on Engineering Management* 40, 180–187.
- U.S. Environmental Protection Agency., 2009. *User’s Guide to MOBILE6.1 and MOBILE6.2*.
- Van Lint, J., Hoogendoorn, S., Schreuder, M., 2008. FASTLANE: new multiclass first-order traffic flow model. *Transportation Research Record* 2088, 177–187.
- Venigalla, M., Chatterjee, A., Bronzini, M., 1999. A specialized equilibrium assignment algorithm for air quality modeling. *Transportation Research Part D* 4, 29–44.
- Wahle, J., Annen, O., Schuster, C., Neubert, L., Schreckenberg, M., 2001. A dynamic route guidance system based on real traffic data. *European Journal of Operational Research* 131, 302–308.
- Wallace, C., Courage, K., Reaves, D., Schoene, G., Euler, G., 1984. *TRANSYT-7F user’s manual*. Technical Report. Center for Microcomputers in Transportation, University of Florida.
- Wang, Y., Kosmatopoulos, E., M.Papageorgiou, I.Papamichail., 2014. Local ramp metering in the presence of a distant downstream bottleneck: theoretical analysis and simulation study. *IEEE Transactions on Intelligent Transportation Systems* 15, 2024–2039.

- Wang, Y., Papageorgiou, M., Gaffney, J., Papamichail, I., Guo., J., 2010. Local ramp metering in the presence of random-location bottlenecks downstream of a metered on-ramp, in: Proc. of the 13th IEEE International Conference on Intelligent Transportation Systems, pp. 1462–1467.
- Wang, Y., Papageorgiou, M., Messmer., A., 2001. Feedback and iterative routing strategies for freeway networks, in: Proc. of the 2001 IEEE International Conference on Control Applications, pp. 1162–1167.
- Wang, Y., Papageorgiou, M., Messmer., A., 2002. A predictive feedback routing control strategy for freeway network traffic., in: Proc. of the American Control Conference, pp. 3606–3611.
- W.Jang, Ran, B., Choi., K., 2005. A discrete time dynamic flow model and a formulation and solution method for dynamic route choice. Transportation Research Part B 39, 593–620.
- Wong, G., Wong., S., 2002. A multi-class traffic flow model - an extension of LWR model with heterogeneous drivers. Transportation Research Part A 36, 827–841.
- Zegeye, S., De Schutter, B., Hellendoorn, J., Breunese, E., Hegyi, A., 2012. A predictive traffic controller for sustainable mobility using parameterized control policies. IEEE Transactions on Intelligent Transportation Systems 13, 1420–1429.
- Zegeye, S., De Schutter, B., Hellendoorn, J., Breunese, E., Hegyi., A., 2013. Integrated macroscopic traffic flow, emission, and fuel consumption model for control purposes. Transportation Research Part C 31, 158–171.

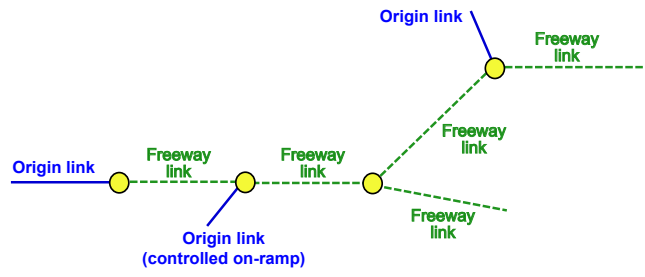


Figure 1: Sketch of the network.

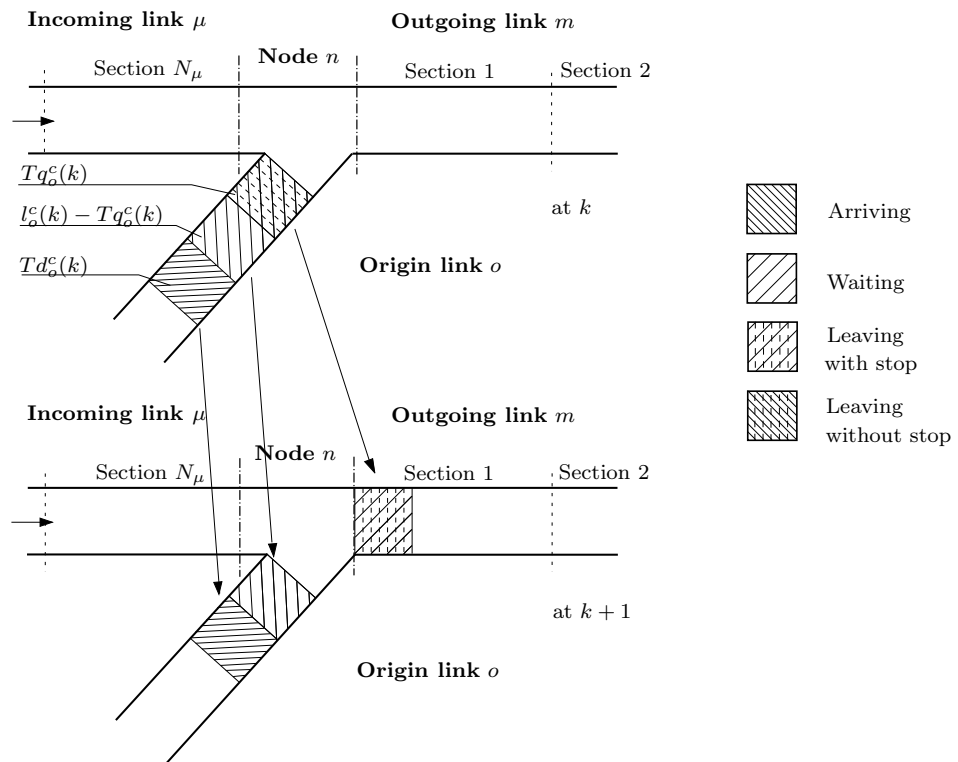


Figure 2: Dynamic behaviour of vehicles at the origin link in case 1.

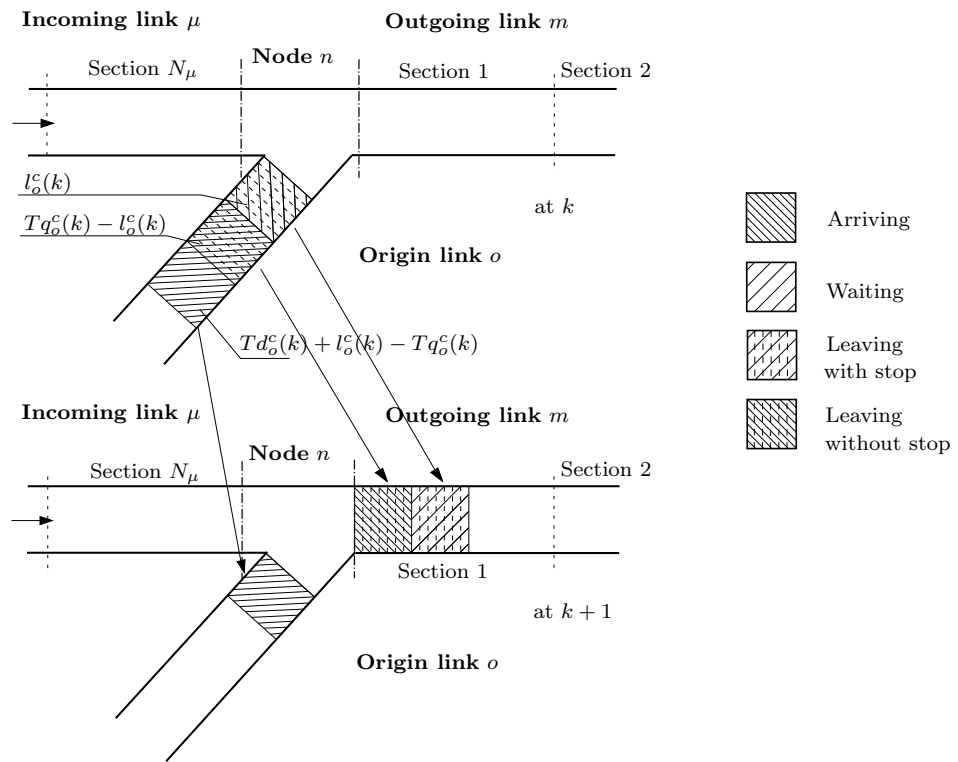


Figure 3: Dynamic behaviour of vehicles at the origin link in case 2.

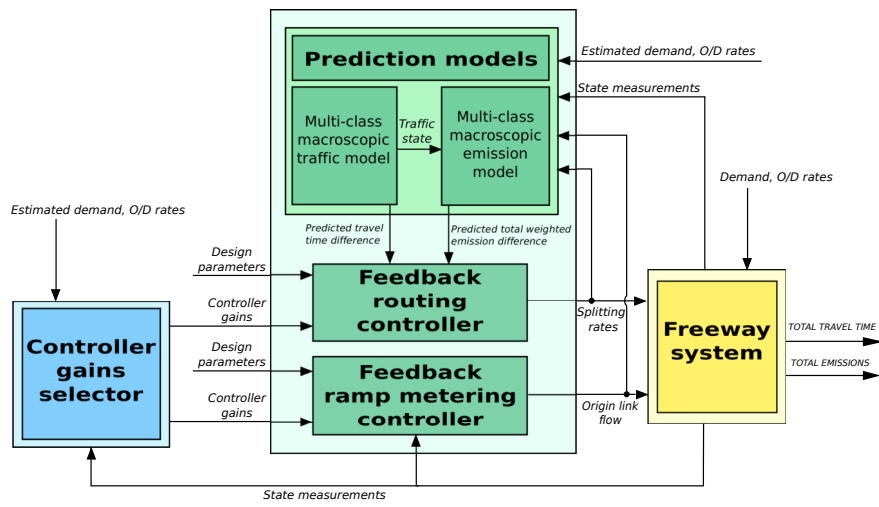


Figure 4: Layout of the control framework.

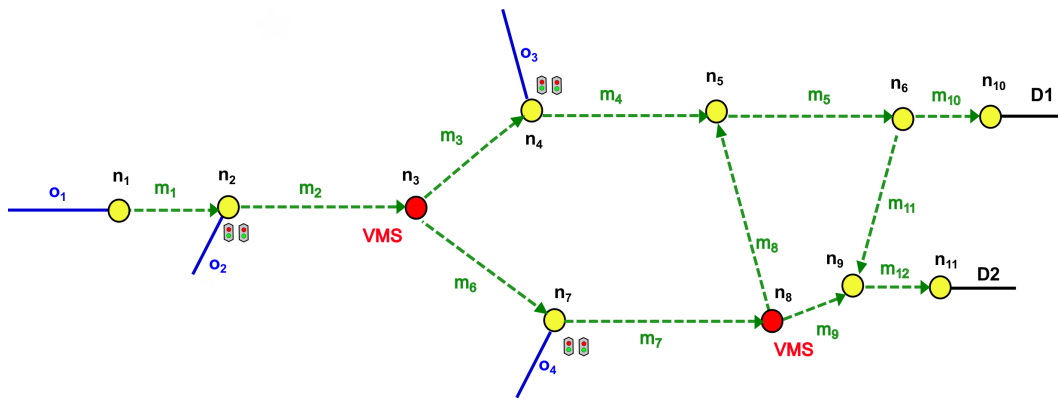


Figure 5: Layout of the case study freeway network.

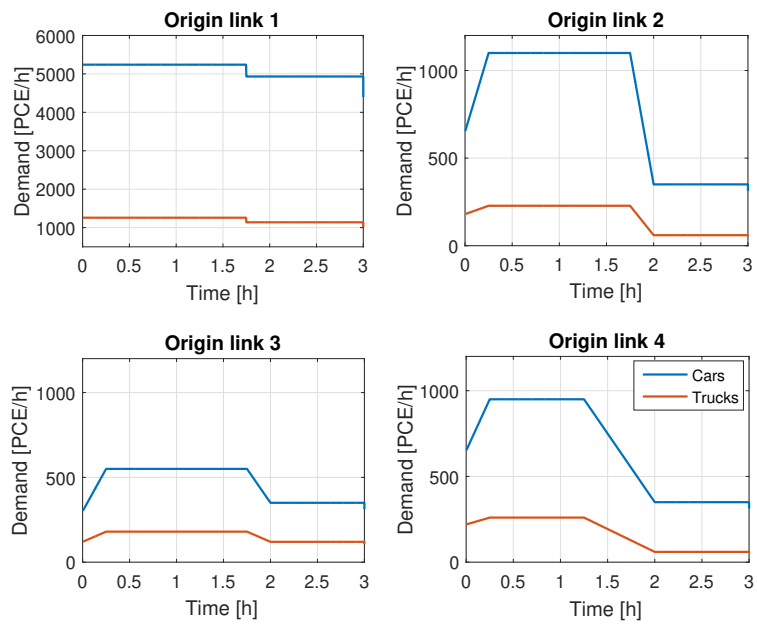


Figure 6: Demands at the origin links.

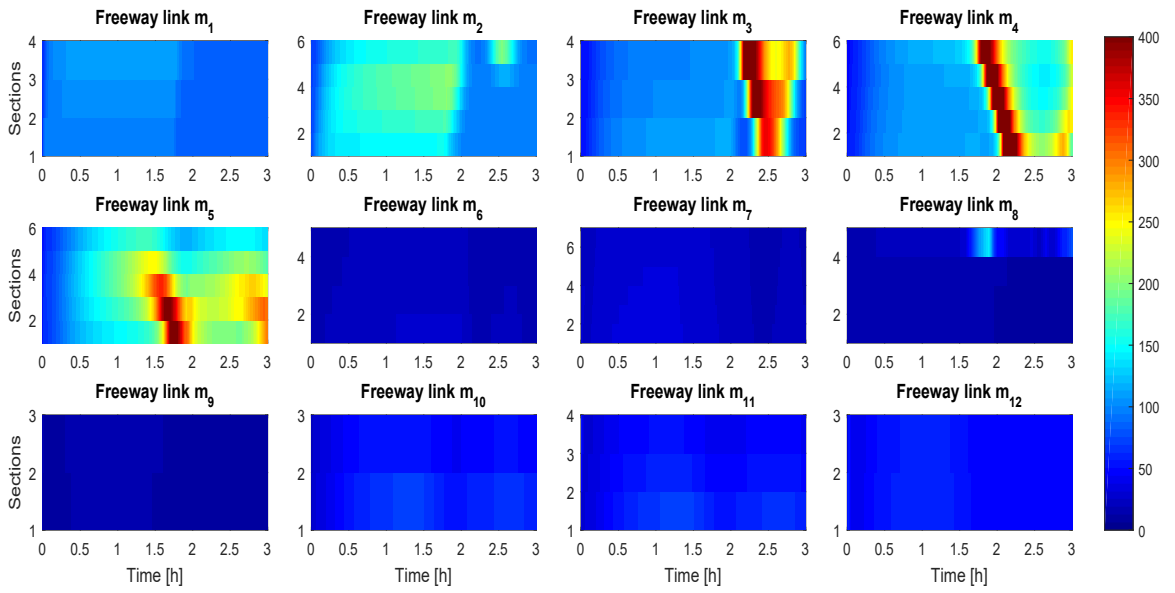


Figure 7: Mainstream density profiles [PCE/km] for each freeway link in the uncontrolled case.

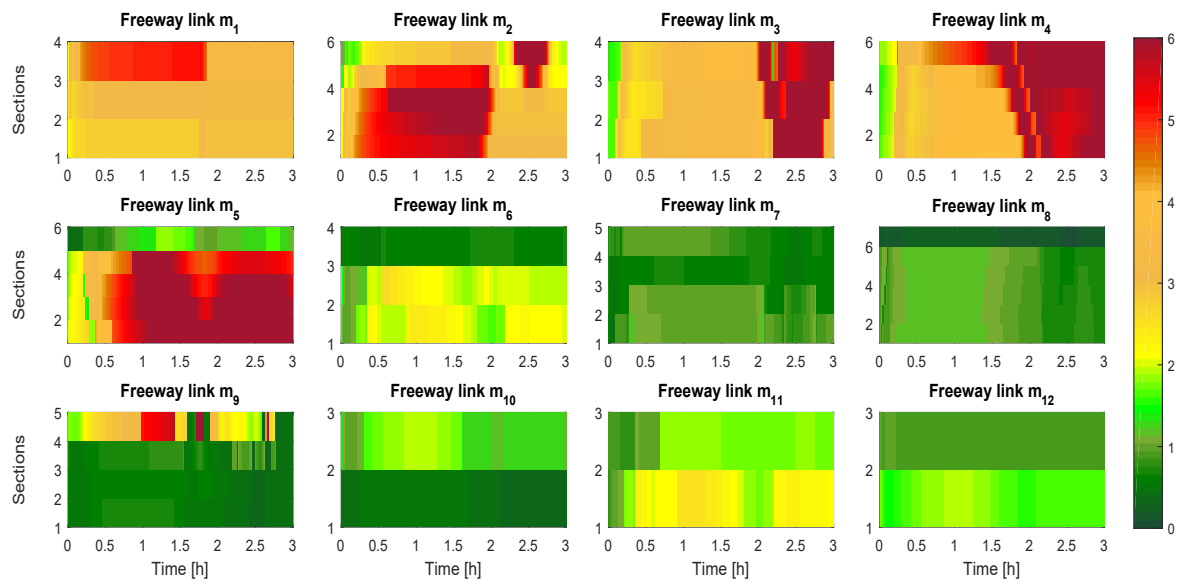


Figure 8: CO₂ emissions profiles [kg] for each freeway link in the uncontrolled case.

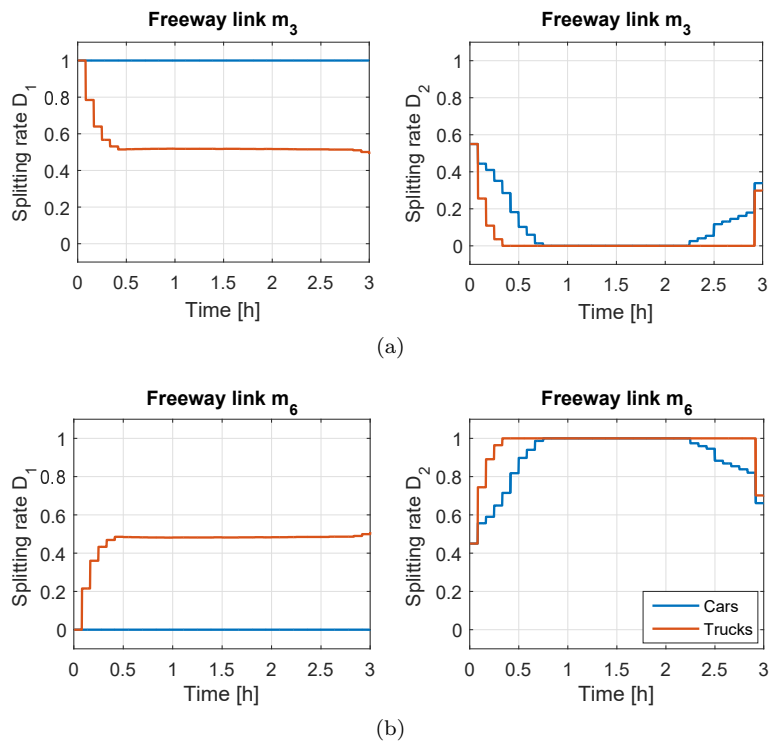


Figure 9: Splitting rates at node n_3 : freeway link m_3 (9a) and freeway link m_6 (9b) - Case 1.

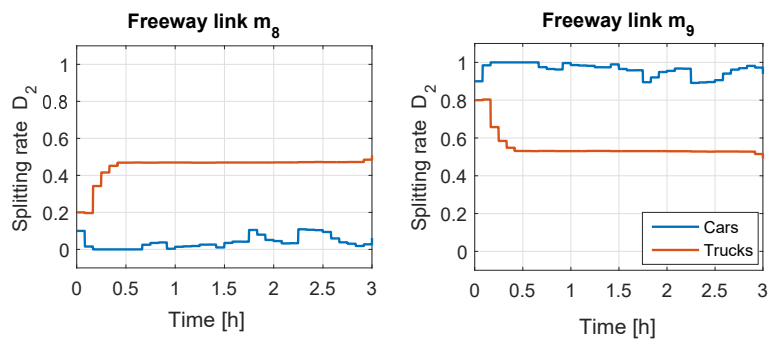


Figure 10: Splitting rates at node n_8 : freeway link m_8 (left side) and freeway link m_9 (right side) - Case 1.

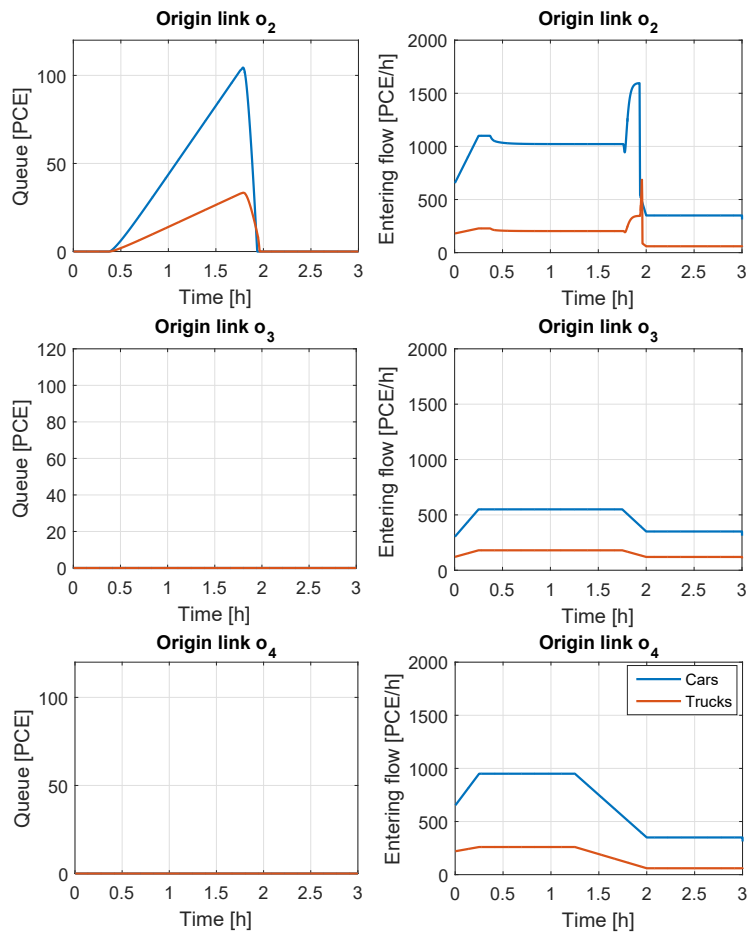


Figure 11: Queue lengths (left side) and entering flows (right side) at the controlled origin links - Case 1.

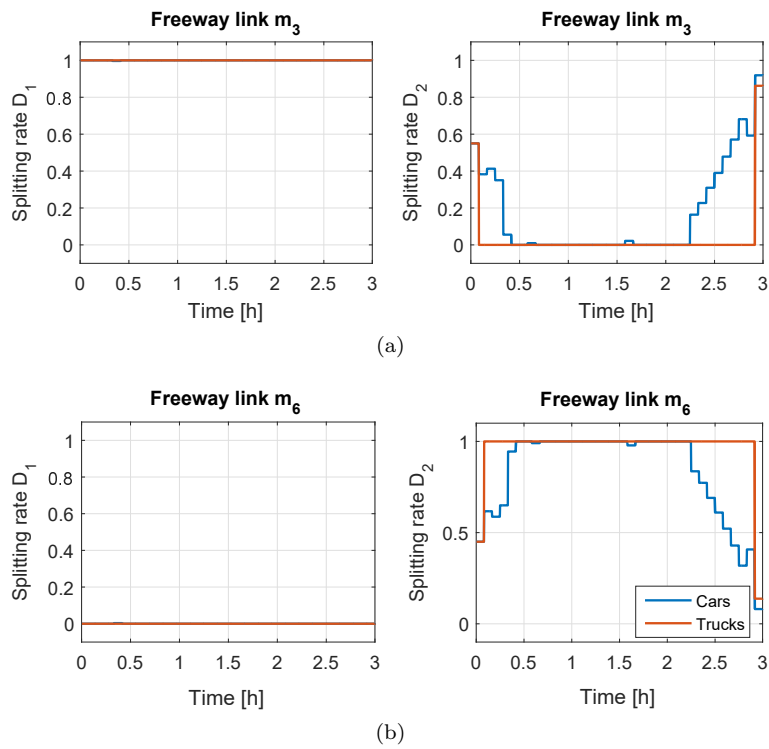


Figure 12: Splitting rates at node n_3 : freeway link m_3 (12a) and freeway link m_6 (12b) - Case 2.

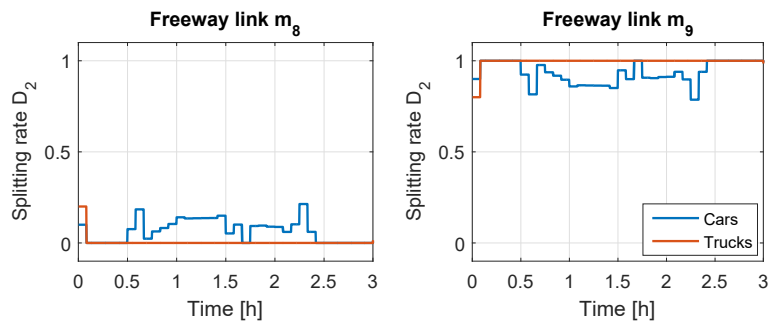


Figure 13: Splitting rates at node n_8 : freeway link m_8 (left side), and at the and freeway link m_9 (right side) - Case 2.

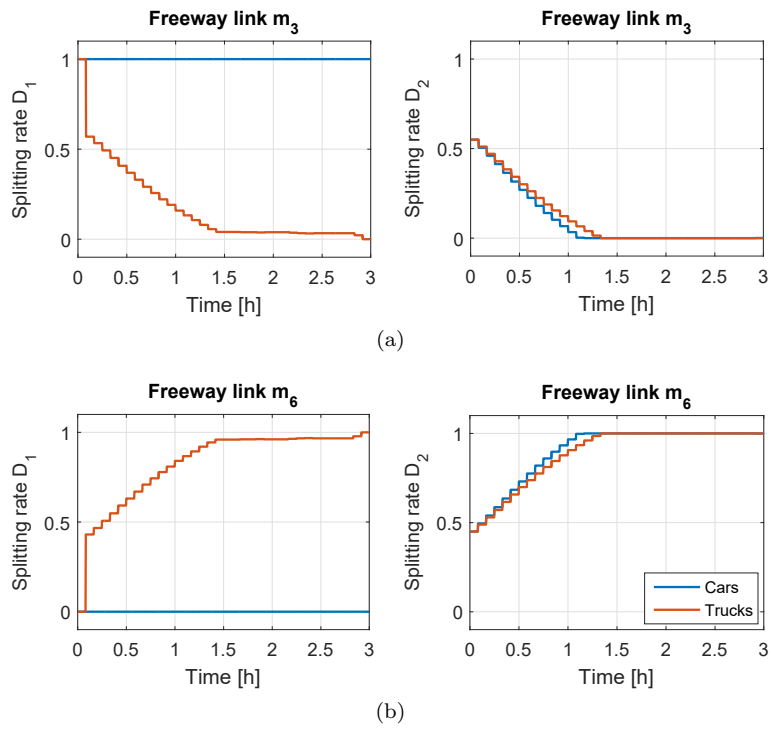


Figure 14: Splitting rates at node n_3 : freeway link m_3 (14a) and freeway link m_6 (14b) - Case 3.

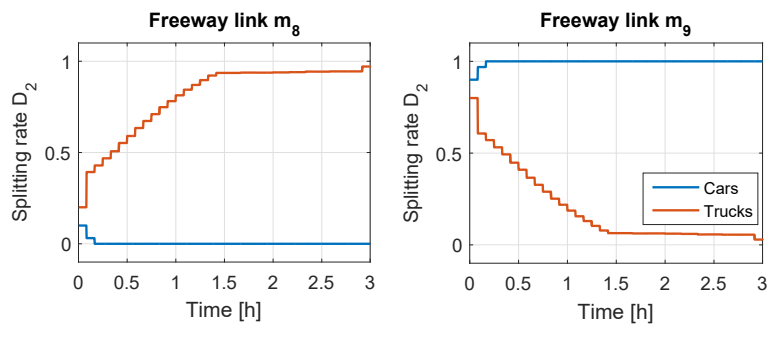


Figure 15: Splitting rates at node n_8 : freeway link m_8 (left side) and freeway link m_9 (right side) - Case 3.

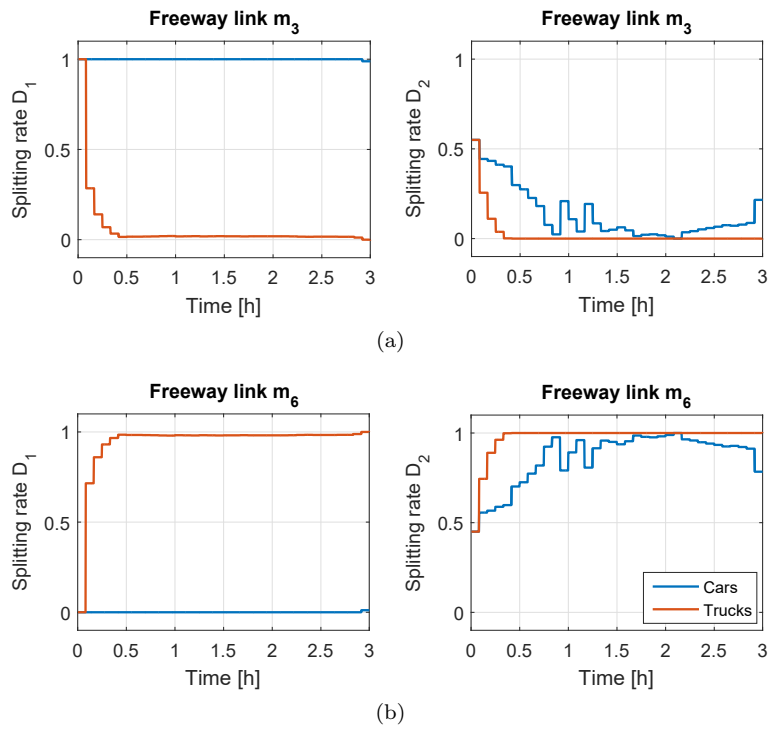


Figure 16: Splitting rates at node n_3 : freeway link m_3 (16a) and freeway link m_6 (16b) - Case 4.

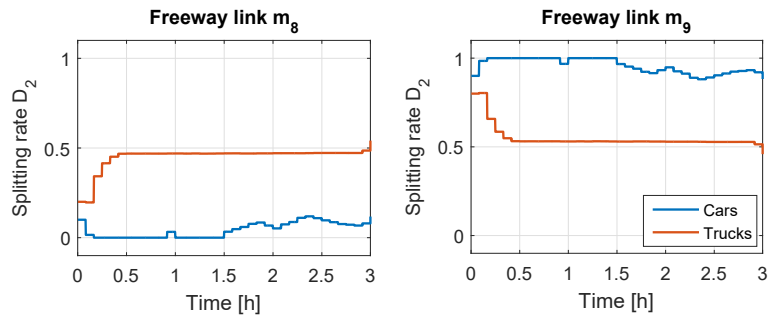


Figure 17: Splitting rates at node n_8 : freeway link m_8 (left side) and freeway link m_9 (right side) - Case 4.

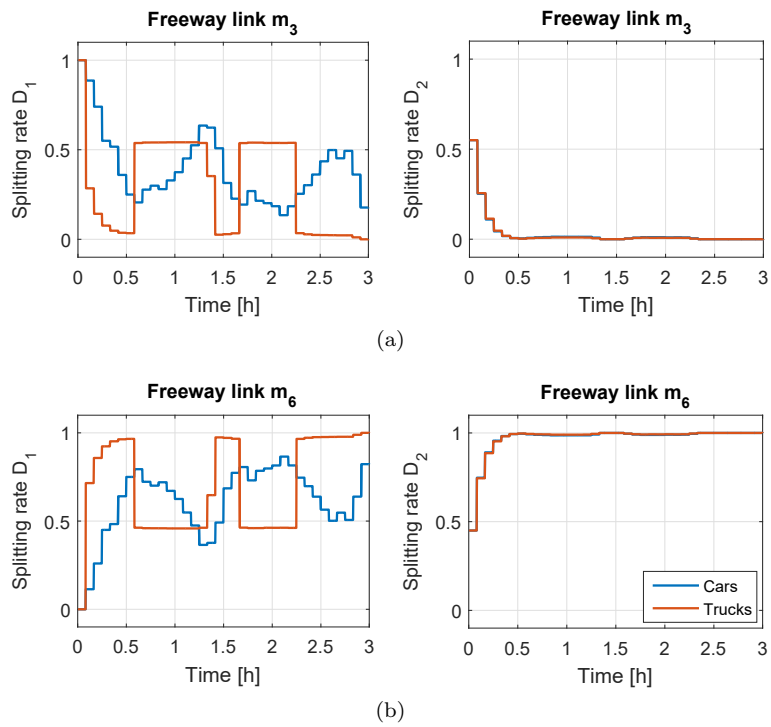


Figure 18: Splitting rates at node n_3 : freeway link m_3 (18a) and freeway link m_6 (18b) - Case 5.

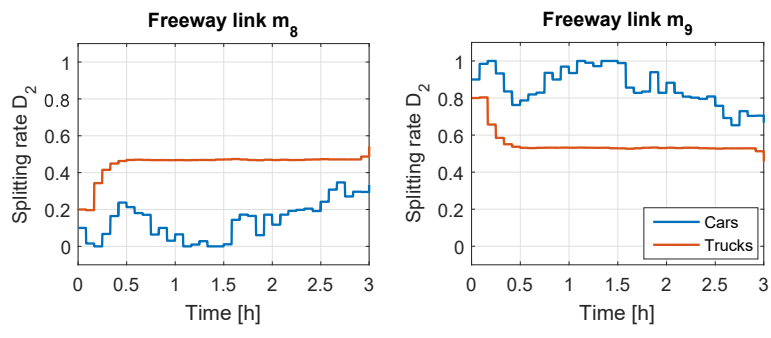


Figure 19: Splitting rates at node n_8 : freeway link m_8 (left side) and freeway link m_9 (right side) - Case 5.

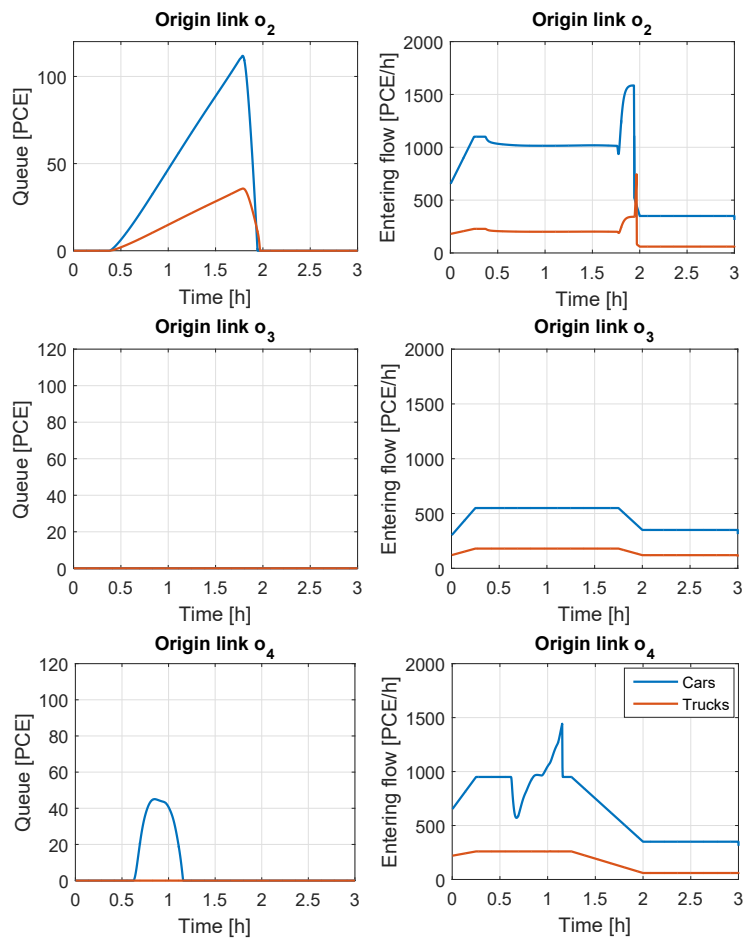


Figure 20: Queue lengths (left side) and entering flows (right side) at the controlled origin links - Case 5.

Table 1: Definition of the variables of the multi-class VERSIT+ model.

VERSIT+	Multi-class VERSIT+		
E	$E_{m,i}^{\text{seg},c}$	$E_{m,i,i+1}^{\text{cross},c}$	$E_o^{\text{orig},y,c}$
w	$w_{m,i}^{\text{seg},c}$	$w_{m,i,i+1}^{\text{cross},c}$	$w_o^{y,c}$
v	$v_{m,i}^c$	$v_{m,i}^c$	$v_o^{y,c}$
a	$a_{m,i}^{\text{seg},c}$	$a_{m,i,i+1}^{\text{cross},c}$	$a_o^{y,c}$

Table 2: Controller gains in the five cases.

(a) Feedback routing controller gains.

Gain	$K_P^{t,1}$	$K_P^{t,2}$	$K_I^{t,1}$	$K_I^{t,2}$	$K_P^{e,1}$	$K_P^{e,2}$	$K_P^{e,1}$	$K_P^{e,2}$
Value	0.3	0.1	0.8	0.5	0.1	0.05	0.3	0.2

(b) Feedback ramp metering controller gains.

Gain	K_P^1	K_P^2	K_R^1	K_R^2
Value	102.1	49.8	33.5	5.7

Table 3: Design parameters and performance indicators in the five cases.

Case	ϕ_3^1	ϕ_3^2	ϕ_4^1	ϕ_4^2	α^1	α^2	$R_{\text{TTS}}[\%]$	$R_{\text{TE}}[\%]$
<i>1</i>	1	1	1	1	0.5	0.5	25.85	27.10
<i>2</i>	1	1	1	1	0	0	26.58	27.91
<i>3</i>	1	1	1	1	1	1	24.23	25.04
<i>4</i>	1	2.5	1	2.5	0.5	0.5	25.32	26.55
<i>5</i>	2.15	2.5	2.15	2.5	0.5	0.5	17.58	17.71